FABRICATION AND CHARACTERIZATION OF ZnS BUFFER LAYER FOR THIN FILM SOLAR CELL USING CHEMICAL BATH DEPOSITION (CBD) METHOD

BY

MD. SHARFUDDIN
ROLL: 7003
REGISTRATION NUMBER: HA- 1530
ADMISSION SESSION: 2014-2015

A THESIS SUBMITTED IN PARTIAL FULFILLMENT FOR THE DEGREE OF

MASTER OF SCIENCE

IN

RENEWABLE ENERGY TECHNOLOGY

INSTITUTE OF ENERGY

UNIVERSITY OF DHAKA

SEPTEMBER 2016

DECLARATION

I hereby declare that this submission is my own work towards the M.Sc. and that, to the best of my knowledge, it contains no material previously published by any person nor material which has been accepted for the award of any other degree of the University, except where due acknowledgment has been made in the text.

Md. Sharfuddin ....

Student Signature Date

RECOMMENDATION CERTIFICATE

We hereby recommend that the project work entitled "**FABRICATION AND CHARACTERIZATION OF ZnS BUFFER LAYER FOR THIN FILM SOLAR CELL USING CHEMICAL BATH DEPOSITION (CBD) METHOD**" carried out under our supervision and guidance by **Professor Dr. Saiful Huque, Muhammad Shahriar Bashar** and **Munira Sultana** may be accepted in the partial fulfillment of the requirements for the degree of "Master of Science" in Renewable Energy Technology. To the best of our knowledge, this work has not been submitted for the award of any other degree or diploma.

| --- | --- | --- |
Professor Dr. Saiful Huque	Muhammad Shahriar Bashar	Munira Sultana
Director	Senior Scientific Officer	Scientific Officer
Institute of Energy	IFRD, BCSIR	IFRD, BCSIR
University of Dhaka		

ABSTRACT

Zinc sulfide thin films were prepared by chemical bath deposition technique using zinc sulfate ($ZnSO_4.7H_2O$) and thiourea [$SC(NH_2)_2$] as sources of Zn^{2+} and S^{2-} ions, and ammonia (NH_3) and hydrazine hydrate (N_2H_4) as complexing agents. ZnS is an important semiconductor compound of excellent physical properties such as wide band-gap energy of 3.7 eV at 300 K, high refractive index (2.35 at 632 nm), transparent to practically all wavelengths of the solar spectrum, non-toxic and environmentally friendly buffer materials that are suitable for industrial production. A very attractive method for producing ZnS thin films, due to the possibility of large-area deposition at low cost is the chemical bath deposition (CBD) method. Chemical bath deposition (CBD) is known to produce solar cell grade films at simpleness, convenience, a low cost and low temperature. The depositions were carried out by varying PH of bath solution from 9.3 to 10.1 and keeping bath temperature fixed at 70 °C for two hours. The thickness of the films was tuned between 72 nm to 319 nm by controlling the ammonia and thiourea concentration. The structural, stoichiometric proportion, morphology and optical properties of the ZnS thin films were investigated as a function of thiourea and ammonia concentrations using X-ray diffraction (XRD), energy-dispersive spectroscopy (EDS), scanning electron microscopy (SEM) and UV- visible spectro-photometry measurements. X-ray diffraction analysis of the as-deposited films showed that the films have amorphous structure and poor crystallinity. Energy-dispersive spectroscopy (EDS) showed that all ZnS thin films exhibited both Zn and S. The UV–visible spectrophotometric measurement showed that, the transmittance of the ZnS thin films vary from 45% to 65%, while the band gap vary from 3.85 eV to 3.89 eV for different ammonia and thiourea concentration.

ACKNOWLEDGMENTS

My deepest gratitude goes to almighty God who endowed me with health, grace, wisdom, patience and direction to bring this project to completion. I fully acknowledge my indebtedness to **Professor Dr. Saiful Huque**, Director, Institute of Energy University Of Dhaka, for his direction, pieces of advice and monitoring during the thesis. I also express my special thanks and gratefulness to my co-guides **Muhammad Shahriar Bashar,** Senior Scientific Officer, IFRD, BCSIR. and **Munira Sultana** Scientific Officer, IFRD, BCSIR. for their kind suggestions and help from time to time. I finally express my sincere thanks to my parents for their financial support, and passionate prayers throughout the entire period.

Table of Contents

LIST OF FIGURES

LIST OF TABLES

Dedicated to my parents

1. CHAPTER ONE

1.0 INTRODUCTION

Energy is the prerequisite for creation of wealth and sustainability of development. The importance of energy in economic development has been recognised historically but the equitable distribution of energy amongst the masses has always been a matter of great concern. The cost of energy really came into the picture in the aftermath of the global oil crisis in the early 1970s. Since then the two key aspects which attracted the global attention are the cost of energy and related impact on our environment.

Sustainability of development can be ensured by use of sustainable energy resources which are environment-friendly and available in abundance. And the only possible answer to this problem is Renewable Energy. Kyoto Protocol echoed the same. The UN also strongly recommends the increase of share of the Renewable Sources in the energy supply mix which, at present, is mere 0.8%. Renewable Sources include wind, biomass, geothermal, hydro-power, ocean thermal and last but not the least Solar.

Owing to the exponential growth of global population, the need for energy is going to be doubled in coming fifty years. But this huge demand can be met by solar energy alone. Available data shows that earth receives 3×10^{24} joule energy per year which is about 10,000 times the present global consumption of energy. In other words, if 0.1% of earth surface is covered with solar cells of 10 % conversion efficiency it would meet our present demand for energy. India receives 6.6×10^{15} kWh annually in terms of solar radiation which, figuratively, 104 times our annual consumption of electricity. The use of mere 1% of this insolation can cater to all energy-related issues in our country. Thus it is needless to say that the huge potential of solar energy has to be explored in order to harness it efficiently and bring it to the use of mankind.

It all started in the year 1839, when a French teenager Alexandra Edmund Bequerel reported the Photo Voltaic Effect for the first time. The major thrust really came in this field of science in the first decade of nineteen hundred when Einstein was awarded with Nobel Prize for his pioneering work in Photoelectric Effect. The pace of research in Photovoltaic and opto-electronics was boosted in the last quarter. With the advancement in the field of nanotechnology and material science, a huge number of motivated researchers are exploring

this vast area of science and thereby making great contribution towards different methods of fabrication techniques to produce a cheap, sustainable, environment friendly, highly efficient solar cell and other nano-electronic devices.

Semiconducting materials play an indispensable role in contemporary electronics. In the early days of radio and television, transmitting and receiving equipment relied on vacuum tubes, but these have been almost completely replaced in the last four decades by semiconducting materials, including transistors, diodes, integrated circuits and other solid-state devices [1]. Such devices have found wide application because of their compactness, reliability, power efficiency, and low cost. As discrete components, they have found use in power devices, optical sensors, and light emitters, including solid-state lasers. They have a wide range of current- and voltage-handling capabilities and, more important, lend themselves to integration into complex but readily manufacturable microelectronic circuits. They are, and will be in the foreseeable future, the key elements for the majority of electronic systems, serving communications, signal processing, computing, and control applications in both the consumer and industrial markets (Encyclopedia Britannica, 2010).

The study of semiconducting materials began in the early 19th century. The elemental semiconducting materials are those composed of single species of atoms, such as silicon (Si), germanium (Ge), and tin (Sn) in group IV and selenium (Se) and tellurium (Te) in group VI of the periodic table. During the early 1950s germanium was the major semiconductor material. However, it proved unsuitable for many applications, because devices made of the material exhibited high leakage currents at only moderately elevated temperatures. Since the early 1960s silicon has become by far the most widely used semiconductor, virtually supplanting germanium as a material for device fabrication. The main reasons for this are twofold: (1) silicon devices exhibit much lower leakage currents, and (2) silicon dioxide (SiO_2), which is a high-quality insulator, is easy to incorporate as part of a silicon-based device. Thus, silicon technology has become very advanced and invasive, with silicon devices constituting more than 95 percent of all semiconductor products sold worldwide.

The potential applications of chalcogenide based materials in electronic and optoelectronic devices are vast, but has received little attention until recently due to the cheap and wide availability of silicon based alternatives [2]. Chalcogenide II-VI, compound semiconductors, such as zinc sulphide (ZnS) has generated a lot of interest among scientists because of its extensive use in the fabrication of solid state devices such as solar cells, thin film transistors and electroluminescent displays.

ZnS is an important II-VI group semiconductor with a large direct band gap of 3.5–3.8eV in the UV range [3]. Zinc sulphide is a white to yellow-colored powder or crystal with molecular mass of 97.474 $gmol^{-1}$ and density of 4.090 gcm^{-3}. It is typically encountered in the more stable cubic form, known also as zinc blende or sphalerite. The hexagonal form is also known both as a synthetic material and as the mineral wurtzite. Both sphalerite and wurtzite are intrinsic, wide-band gap semiconductors. The cubic form has a band gap of 3.54 eV at 300 K whereas the hexagonal form has a band gap of 3.91 eV (Wells, 1984). ZnS has a melting point (phase transition) of 1020 ^{o}C. The cubic form is stable at room temperature, while the less dense hexagonal form (wurtzite) is stable above 1020 ^{o}C at atmospheric pressure [4].

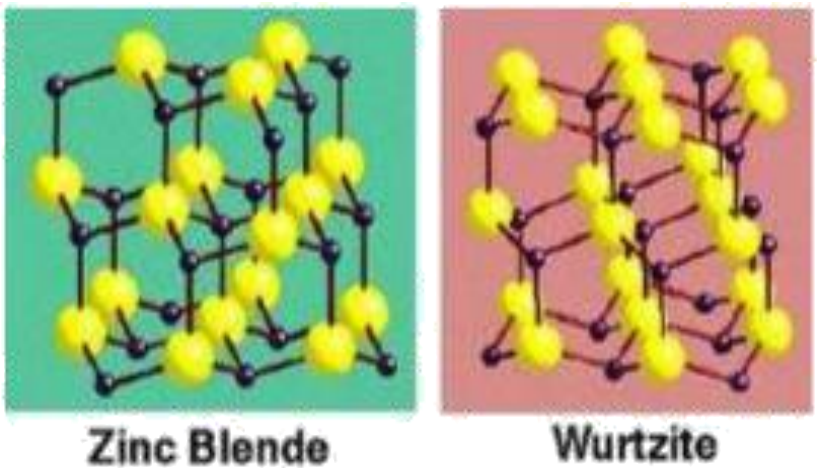

Figure 1.1 Shows Each Crystal Structure

Figure 1.1 shows the sphalerite or zinc blende and the wurtzite crystal structure of ZnS (chem.ox.ac.uk)

The sphalerite structure can be derived from a cubic close packing of ions, while the wurtzite structure is derived from a hexagonal close packing scheme. This situation is not that simple however, because the difference in energy of the two structures is small. Arterton*et al.*, (1992) reported that electroluminescent material must contain both sphalerite and wurtzite phases. The wurtzite type structure predominates when the bonding is primarily ionic whereas the more covalent systems favor the sphalerite form. The nature of the end product is

usually dependent on heat treatment temperature, cooling profile, and cooling atmosphere. One phase can be more suitable than another in certain applications. The cubic phase of ZnS is not grown as easily as the hexagonal phase, thus making the hexagonal phase more appealing for electroluminescence device applications (Bellotti*et al.,* 1998). ZnS was used by Ernest Rutherford and others in the early years of nuclear physics as a scintillation detector, because it emits light on excitation by X-rays or electron beam, making it useful for X-ray screens and cathode ray tubes. It also exhibits phosphorescence due to impurities on illumination with blue or ultraviolet light [5].

ZnS thin films have been found valuable in various devices. The application of ZnS thin films which cover a wide area of interest are. Antireflection coating for the solar cell [6]. Environmental friendly buffer layer as compared to CdS layer in CIS based thin film solar cell [7]. Wide band gap material for electroluminescent and optoelectronic devices (Tong *et al.,* 1996), Photosynthetic coating [8], Blue light emitting laser diodes [9], As α- particle detector [10].

In thin film solar cells based on $CuGaIn(S, Se)_2$ absorbers, a CdS (Cadmium Sulphide) buffer layer is generally required in order to obtain high conversion efficiency. However, there are toxic hazards with respect to the production and use of the CdS layer. Therefore research in developing Cadmium (Cd) free buffer layers has been encouraged. This has lead to the investigation of ZnS as a buffer layer in ZnO / ZnS / $CuInS_2$ devices [11]. ZnS has a wider energy band gap than CdS, which results in the transmission of more high-energy photons to the junction, and to the enhancement of the blue response of the photovoltaic cells.

Zinc sulphide (ZnS) thin films with a wide direct band gap and n-type conductivity are promising for optoelectronic device applications, such as electroluminescent devices and photovoltaic cells. In optoelectronics, it can be used as light emitting diode in the blue to ultraviolet spectral region due to its wide band gap of 3.7 eV at room temperature [12]. In the

area of optics, ZnS can be used as a reflector and dielectric filter because of its high refractive index (2.35) and high transmittance in the visible range, respectively.

In recent times, the study of semiconductors in the bulk has been replaced with that of thin films. Thin film technique is one of the most fully-fledged technologies that greatly contribute to developing the study of semiconductors by giving a clear indication of their chemical and physical properties. Thin films have mechanical, electrical, magnetic and optical properties which may differ from those of the bulk material and are used commonly in the form of a deposit on a suitable substrate. Presently, rapidly changing needs for thin film materials and devices are creating new opportunities for the development of new processes, materials and technologies.

There exists a huge variety of thin film deposition processes and technologies which originate from purely physical or purely chemical processes. These include vacuum evaporation, spray pyrolysis, sputtering molecular beam epitaxy, vapor phase epitaxy, chemical vapor deposition, solution growth, screen printing and electrophoresis. Despite the existence of these large variety of deposition techniques, searching for the most reliable and economic deposition technique has always been the main goal. Of all the techniques mentioned chemical bath deposition is currently attracting a great deal of attention as the techniques is relatively simple and cost effective, has minimum material wastage, does not need sophisticated instrument and vacuum, and can be applied in large area deposition at low temperature. This method uses a controlled chemical reaction to deposit a thin film. In the typical experimental approach, the substrates are immersed in solution containing the Chalcogenide source, metal ion, and complexing agent [13].

To make semiconducting thin films useful in any given applications, it is very important to investigate their optical properties. Optical properties are directly related to structural and

electronic properties of solids, and hence very important in device applications. A detailed knowledge of optical properties can provide a huge amount of information about their structure, optoelectronic behavior, transport of charged carriers, etc. [14]. These are important parameters for scientists and technocrats to decide its end use.

This thesis is primarily concerned with the fabrication, characterization and the optical properties of zinc sulphide thin films deposited from chemical baths.

1.1 OBJECTIVES OF THE PROJET

Presently the solar-cell-market is dominated by monocrystalline and polycrystalline silicon solar cells. The major setback for using these materials is their very high cost of production. Economics of energy production suffer from this. Again, owing to their indirect band-gap, these materials are not ideal for fabricating the absorber layer of the solar cell. As for materials with indirect band-gap the absorption of solar radiation is much inefficient as compared to the materials having direct-band gap. Therefore thick layer of such indirect-band gap-materials is required to produce the desired output and hence the economy of energy production suffers.

The per unit cost of electricity generation from solar cell is the major hindrance in adopting solar power as a popular source of energy as compared to other conventional technologies of power generation. Therefore the need-of-the-hour is to develop new materials and explore new technologies in order to curtail the cost per watt peak of solar photovoltaic power conversion.

Thin films greatly reduce the amount of semiconductor material required for each cell when compared to silicon wafers and hence lowers the cost of production of photovoltaic cells. Gallium arsenide (GaAs), copper, cadmium telluride (CdTe) indium diselenide ($CuInSe_2$) and titanium dioxide (TiO_2) are materials that have been mostly used for thin film PV cells [3]. These materials have some inherent problems. Thus to study ZnS buffer layer as a strong contender in thin film technology has really been the main aim of the present work.

In thin film solar cell technology, the major function of the buffer layer (*p* or *n* type) is to create the junction with the absorber layer with minimum absorption losses and to drive the

generated carries to the electrode. The overall efficiency of the cell depends greatly upon this buffer layer (or window layer) ZnS, being a high bandgap material, thus has become a promising material for heterojunction thin film solar cell technology as buffer layer. No toxicity, availability, high direct band-gap etc. are some of the major advantages of ZnS. Several technologies for fabricating ZnS thin film has been explore till date.

The research presented in this thesis was motivated by the following objectives:

- To deposit zinc sulphide (ZnS) thin films using chemical bath deposition method containing zinc sulfate ($ZnSO_4.7H_2O$), thiourea[$SC(NH_2)_2$], ammonia (NH_3) and hydrazine hydrate (N_2H_4).
- To investigate the optical properties, morphology, structure and elemental composition of the thin films.
- To analyze optical band gap of the thin films with different molar concentration of ammonia (NH_3) and thiourea [$SC(NH_2)_2$].

1.2 THIN FILM

In simple terms the word thin film means the layer of a material whose thickness vary in the range from few nanometers to several micrometers. Thin films find wide range of applications namely- electronic semiconductor devices, optical coatings, pharmaceuticals etc. apart from the most common PV solar cell fabrication.

As far as fabrication technologies of thin film goes, it can be broadly classified under two distinct categories- physical method and chemical method. Thermal evaporation in vacuum, molecular beam epitaxy, sputtering, pulsed laser deposition etc. are some of the widely used Physical methods whereas – Electrochemical Deposition (ECD), Chemical Bath Deposition (CBD) and Successive Ionic Layer Absorption Reaction (SILAR) method etc. are the commonly used Chemical Methods.

1.2.1 ZNS AS A BUFFER LAYER

Thin layers of ZnS have been successfully used as a substitute to the highly toxic CdS buffer layer in heterojunction solar cells and photovoltaic devices with conversion efficiencies >15%. It is also interesting to use ZnS as a window material in order to exploit its wide band gap to increase the blue response of the solar cell device further and reduce the interface

defects. If ZnS is to be used as a window layer in solar cells, its electrical resistivity is to be decreased by several orders of magnitude as undoped ZnS layers are highly resistive in nature with the electrical resistivity of ~$10^7\Omega$cm. An effective way to decrease the electrical resistivity of ZnS films is to dope the layers by suitable dopants such as Al, Ga and Cu without affecting its optical behavior.

1.2.2. WHY ZnS?

The ZnS-based buffer layer is one of the most popular candidates for replacing the CBD CdS. This buffer demonstrated the highest CIGS-based solar cell efficiencies, is nontoxic and is relatively less costly.

Certain properties pertaining to ZnS are unique and advantageous:

- Non-toxic nature
- Environment friendly
- It belongs to the group of II-VI compounds.
- It is a n-type semiconductor material ZnS has a direct band-gap.
- It has the largest band-gap amongst group II-VI compounds.
- ZnS is also important because of its higher transmission, high refractive index, and linear and nonlinear absorption, indicating that it finds wide applications in optoelectronic fields as deep-blue light emitting devices or a base material for phosphors.
- ZnS has a larger bandgap of 3.72 eV and 3.77 eV (for cubic zincblende (ZB) and hexagonal wurtzite (WZ) ZnS, respectively. Therefore it is more suitable for ultraviolet (UV)-light based devices such as sensors/ photo detectors. On the other hand, ZnS is traditionally the most suitable candidate for electroluminescence devices.
- High optical transmittance of >85% in the visible region that can enhance the blue response of the device.

1.3 JUSTIFICATION OF THE PROJECT

Efforts have been made currently for finding new materials for low cost energy conversion. Among the materials of recent research interest are CdS, CdSe, ZnSe, ZnS, etc., which fall in the group of II-VI family of compounds [15], due to their photo- and electro- luminescence

properties and promising applications in optoelectronics. The recent surge of activity in wide band gap materials like ZnS has arisen from the need for electronic devices operating at high power levels and high temperatures. ZnS is an attractive material due to its properties like direct band gap and transparency over a wide range of the visible spectrum.

1.3.1 REASONS FOR CHOOSING THE CHEMICAL BATH DEPOSITION TECHNIQUE

There is considerable interest in the deposition of compound semiconductors by methods which involve relatively low capital expense and are technically undemanding on the experimentalist. One process to meet these criteria is Chemical Bath Deposition (CBD). Such processing methods are particularly appropriate for the production of devices for which large areas substrates and low cost are essential such as solar cells. The CBD method is hugely attractive since the technique possesses a number of advantages over conventional thin-film deposition methods. The main advantages of the CBD method are low cost, low evaporation temperature and easy coating of large surfaces. In addition, this method is free of many inherent problems associated with high-temperature techniques; these problems include increased point defect concentrations, evaporation and decomposition of ZnS thin films.

1.3.2 WHY INVESTIGATE THE OPTICAL PROPERTIES, STRUCTURE, AND MORPHOLOGY OF THE THIN FILM

Several authors have reported the deposition of zinc sulphide thin films containing various chemicals of varying concentrations and under different deposition conditions. However, semiconductor devices based on thin films strongly depend on the structural and optical properties of films obtained from various experimental conditions such as temperature, pH of the solution, stirring and rate of deposition. These conditions can cause the structural and optical properties of films as well as qualities, such as distribution of states within the film to differ, and hence the need to investigate these properties for any preparatory method used.

2. CHAPTER TWO

2.0 LITERATURE REVIEW

The solids known as semiconductors have been the subject of very extensive research over recent decades, not simply because of their intrinsic interest but also because of ever more numerous and powerful applications: rectifiers, transistors, photoelectric cells, magnetometers, solar cells, reprography, lasers, and so forth.

Starting with the development of the transistor by *John Bardeen, Walter Brattain and William Shockley at Bell Telephone Laboratories in 1947*, the technology of semiconductors has exploded. With the creation of integrated circuits and chips, semiconductor devices have penetrated into large parts of our lives. The modern desktop or laptop computer would be unthinkable without microelectronic semiconductor devices, and so would a myriad of other devices [16].

In recent times, the study of semiconductors in the bulk has been replaced with that of thin films. Involvement with thin films dates to the metal ages of antiquity. As a modern science, thin films have been prepared ever since vacuum systems first became available, but deposition as a means of producing films for device purposes is a development of the past 40 years. Thin metallic film coatings on glass or plastic were among the first to be exploited for optical purposes, ranging from mirrors to sunglasses, and this still continues as a major, typically high vacuum, high throughput business.

Semiconductor thin film technology has attracted much attention, because of its matchless size dependent properties and applications in the optoelectronics devices, solar cells, sensors and laser materials. As thin film deposition processes have developed very rapidly over the

past 25 years, particularly in the context of semiconductor devices, processes have become highly specialized [17].

Sulphide thin films such as zinc sulphide (ZnS) has generated a lot of interest among scientists because of its extensive use in the fabrication of solid state devices. There is a diverse range of applications of thin films of this semiconductor and this is reflected in the large amount of literature available on its properties reported by various authors using different deposition techniques.

In [18] successfully produced semiconductor thin films of copper sulphide (CuS) and zinc sulphide (ZnS) on glass microscope slides at 320 K and pH values of 7, 9, 10, 11 and 12 using improved chemical bath deposition method. The results show that pH increases with the optical and solid-state properties (such as transmittance, energy gap, refractive index, absorption coefficient, dielectric constant, thickness and so on) of the films.

The results obtained by [19], the optical absorbance of ZnS thin films for wavelengths in the infrared (up to 1100 nm) and visible spectrum showed that ZnS is practically non-absorbing in these regions. Similar behavior was observed by [20] in the visible region. ZnS films deposited on the glass substrate at room temperature have shown an enhanced absorption in the neighborhood of $\lambda = 330$nm [21] and were expected to have a fine grained structure. The absorption peak shifts towards longer wavelength with increasing thickness. [8] also observed that some ZnS films have high absorbance (~ 0.56) in the near infrared and low absorbance (~ 0.01 – 0.1) in the ultraviolet and visible region.

In 1951, Rood reported that rapidly evaporated ZnS films had a high optical absorption and claimed that the deposition rate for producing good quality films should be about 0.16 nms^{-1}. [22] found that the rapidly deposited ZnS films (1.6 nms^{-1}) had considerable light absorption, but the films formed at about 0.5 nms^{-1} had negligible absorption. He claimed that large ZnS

crystals are formed at high deposition rates and this increased the amount of light lost by scattering within the film. The result was opposite to the general experience because the grain size of most substances falls as the rate of deposition increases. Decomposition of evaporant may explain the greater light absorption of rapidly deposited ZnS thin films. At high rates of evaporation corresponding to high source temperature, free zinc atoms may be trapped in the condensed film. At low evaporation rates decomposition may be less and there is also ample opportunity for free zinc atoms to oxidize either at the condensing surface or in the region of the source. Zinc oxide has a refractive index comparable to that of ZnS and if present in the deposit would not be easily detected.

ZnS films prepared by [23] using resistive heating technique had high transmittance (60–99 %) in the visible and near infrared region. ZnS thin films coated on *Ge* using ionized cluster beam (ICB) method were found to have a transmittance of 96 %. So they are useful as an antireflection coating for the optical transmission window. [24] deposited the (Cd, Zn)S thin films on Corning 7059 glass substrate using chemical bath deposition (CBD) technique for photovoltaic devices. Thin films with zero concentration of Cd demonstrated more than 70 % transmittance at Wavelengths longer than 600 nm. ZnS films grown by [8] had high transmittance (~ 64–98 %) in the visible and near infrared regions. He also observed that some of the films had low transmittance (~ 30–37 %) in near infrared region and high transmittance (~ 78–98 %) in the visible and ultraviolet region. The transmittance of ZnS films grown on polyester foils [25] using successive ionic layer adsorption and reaction method was more than 60 % above 400 nm.

In, [9] It has been reported that ZnS films deposited at high rates and low pressures are found to exhibit bulk values of refractive index when evaporated at room temperature. [20] observed that the refractive index for thinner ZnS films were lower than those for thicker films. The presence of voids, more marked in the thinnest films gave rise to the mean

refractive index below that of bulk material. [22-23] found that refractive index vary with the wavelength of the incident light, whereas for the films analyzed by *Nesmelov et al., (1984)* refractive index seems to be dependent on the growth rate. The refractive index of bulk ZnS is 2.4 [26].

[25] grew ZnS thin films using successive layer adsorption and reaction (SILAR) technique on soda lime glass, ITO - and Al_2O_3 - covered glass and Si substrate and found that the films were inhomogeneous and of poor quality. According to them, the XRD analysis showed that their ZnS films were polycrystalline and presumably cubic. The refractive indices varied from 2.07 to 2.19 on glass grown ZnS films and from 2.15-2.30 on ITO – covered glass.

In 1960, W. Crawford Dunlap, Jr. estimated the band gap ZnS by means of photoconductivity and optical process and came out with 3.67 eV and 3.58 eV respectively. He attributed the difference in energy gap to experimental error or to a temperature difference in band gap, amounting to $3x10^{-4}$ $eV.K^{-1}$.

2.1 PRINCIPLES OF CHEMICAL BATH DEPOSITION (CBD)

As mentioned in chapter one, CBD method is most commonly used because it is a very simple, cost effective and economically reproducible technique that can be applied in large area deposition at low temperature. Chemical bath deposition is used to deposit thin films of a wide-range of materials [27]. The deposition mechanism is largely the same for all such materials. A soluble salt of the required metal is dissolved in an aqueous solution, to release cations. The non-metallic element is provided by a suitable source compound, which decomposes in the presence of hydroxide ions, releasing the anions. The anions and cations then react to form the compound [28]. The source materials used in this work were zinc chloride ($ZnCl_2$) and thioacetamide (C_2H_5NS).

This technique is based on the controlled release of metal ion (M^{2+}) and sulphide (S^{2-}) or selenide (Se^{2-}) ions in an aqueous bath in which the substrates are immersed. In this process, release of metal ion (M^{2+}) is controlled by using a suitable complexing agent. The deposition begins with nucleation phase followed by growth phase in which the thickness of film increases with duration up to the terminal phase where film depletion into constituent ions occurs after a certain time.

Typical CBD processes for sulphides employ an alkaline medium containing the chalcogenide source, the metal ion and added base. A chelating agent is used to limit the hydrolysis of the metal ion and impart some stability to the bath, which would otherwise undergo rapid hydrolysis and precipitation. The technique under these conditions relies on the slow release of ions into an alkaline solution in which the free metal ion is buffered at a low concentration. There are a few reports of the CBD of the binary ZnS [7-8, 29]; the most convincing studies demonstrate that the production of good quality thin films is very difficult by conventional chemical bath systems (Al-Kuhami et al, 2000) due to the stability of hydroxyl species. Unlike, cadmium and lead chalcogenides in which the formation of hydroxide species in solution is an important factor for the formation of high quality films, ZnS is not favored with the hydroxide formation. The relatively small difference in the solubility products of zinc sulphide and zinc hydroxide leads to possible competition between the formation of sulphide and hydroxide in alkaline solutions, with the presence of significant quantities of oxides or hydroxides observed in CBD zinc sulphide films [11,30]. For this reason, hydroxide formation needs to be minimized in order to form quality CBD zinc sulphide thin films [31]. This has led to development of a more favourable medium for formation of ZnS thin films.

In, [11] the author developed the deposition of ZnS from acidic solutions in which urea hydrolysis is used to control the pH and produced among the best ZnS films reported to date.

Roy et al. prepared ZnS films using tartaric acid and hydrazine hydrate as complexing agents [32], whereas Long et al. used tri-sodium citrate and hydrazine hydrate [33]. Agawane et al. [34] and Vallejo et al. [35] used tri-sodium citrate and ammonia. However, ammonia and hydrazine hydrate are still popular choices for complexing agents [36-38,39]. Dona and Herrero reported that the quality and growth rate of ZnS thin films were improved by addition of hydrazine hydrate to a reaction system containing ammonia [32]. Oladeji and Chow observed a lack of film growth if hydrazine hydrate or ammonia was used as the only complexing agent [38].

Two distinct models (ion-by-ion and cluster-by-cluster) have been discussed for the CBD growth mechanism [34, 40]. The reaction mechanism for CdS thin films is believed to be ion-by-ion growth. Although there have been many studies of CBD-ZnS, no definitive mechanism has been established. Some researchers have proposed that ZnS film growth entails adsorption of colloidal particles from solution onto the substrate (cluster-by-cluster mechanism) [41,42] but others suggested that the growth mechanism involves heterogeneous nucleation on the substrate surface and subsequent growth of nuclei in an ion-by-ion process [43,44]. The morphology, stoichiometric composition and structure of ZnS thin films strongly depend on the growth mechanism. ZnS thin films with differing morphology, such as fibrous-like [45], micro scale [46] and Nano scale structures [47,48], have been obtained by CBD.

We prepared ZnS thin films by CBD using ammonia and hydrazine hydrate as complexing agents, and zinc sulfate and thiourea as sources of Zn^{2+} and S^{2-} ions. The effects of thiourea and ammonia concentrations on the surface morphology, optical properties and deposition mechanism for ZnS thin films were investigated. We previously observed that hydrazine hydrate is always necessary to obtain ZnS and ZnSe thin films by CBD [49]. However, the exact role of hydrazine hydrate in the chemical deposition of ZnS and ZnSe thin films remains uncertain. We hypothesized that hydrazine hydrate might play a complexing and/or

catalytic role in the deposition process and thus improves the growth rate, compactness and adherence of CBD-ZnS and -ZnSe thin films.

2.2 CLASSIFICATION OF SOLIDS

There are diverse ways of classifying solids, but perhaps the most useful division is into crystalline, polycrystalline and amorphous. Each type is characterized by the size of an ordered region within the material. An ordered region is spatial volume in which atoms or molecules have a regular geometric arrangement or periodicity. **Figure 2.1** shows the three structural orders [50]. It should be noted that the majority of semiconductors used in electronic applications are crystalline materials, although some polycrystalline and amorphous semiconductors have found a wide range of applications in various electronic devices, [51].

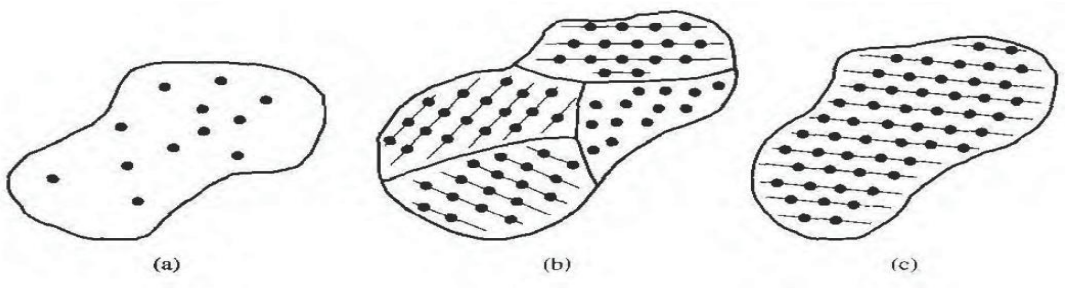

Figure 2.1 Schematics of the three general types of structural orders
(a) amorphous, (b) polycrystalline, (c) crystalline

2.2.1 CRYSTALLINE SEMICONDUCTORS

In crystalline materials, the atoms are arranged in a periodic, regularly repeated three-dimensional pattern—thus presence of long-range order. The universe of traditional solid state physics is defined by the crystalline lattice. The principal actors are the elementary excitations like phonons, polarons, magnons etc. in this lattice. Another is the electron that is

perhaps the principle actor in all of solid state physics. By electron in a solid we mean something a little different from a free electron [16].

A. H. Wilson showed in 1931 how the electronic band theory of crystals developed by F. Bloch can be applied to the understanding of semiconductors. Properties such as the negative temperature coefficient of electrical resistivity follow naturally from Wilson's theory. The key ingredients are the Bloch states which are the Eigen states of an electron moving in the periodic potential of a crystal. The energies of the Bloch states cannot take on all possible values, but are restricted to certain allowed regions or bands separated from one another by forbidden regions called band gaps or energy gaps. Band theory and its outcome-effective mass theory-has allowed us to understand the difference between metals, insulators and semiconductors and how electrons respond to external forces in solids [52].

Information about the structure of solids can be obtained by plotting the so-called radial distribution function, which is the probability, *P(r)*, of finding an atom at a distance *r* from a given atom. In crystalline solids, such a radial distribution function exhibits series of sharp peaks indicative of the long-range order. The curve representing an amorphous material indicates the presence of the short-range order only. This also implies that the number of nearest neighbors to any given atom, on average, is not much different from the corresponding number in the crystalline material.

The electronic band structure of crystalline semiconductors is substantially different from that in the amorphous semiconductors. In crystalline materials, the periodicity of the atomic structure and the presence of long-range order result in a band structure with allowed and forbidden electronic levels, with sharp band edges and a fundamental energy gap separating valence band from the conduction band. In amorphous semiconductors, there is still a fundamental energy gap based on the short-range bonding between the atoms; however, the

sharp band edges of the crystalline semiconductor are replaced in the amorphous materials by exponential band tails due to localized states related to the structural disorder (i.e., bond length and bond angle deviations that broaden the distribution of electronic states); in addition, defects (i.e., dangling bonds) introduce electronic levels in the energy gap [51]. From observations and measurements we find that it is the regular crystalline structure that leads to certain special properties and behavior of the associated materials [53]. The advantage of crystalline material is that, in general, its electrical properties are superior to those of a nonsingle-crystal material, since grain boundaries tend to degrade the electrical characteristics [53].

[54] reported a new, simple and lost cost process to prepare large-scale single crystalline ZnS nanowires based on thermal evaporation of sulfide powders under controlled conditions with the presence of Au catalyst. Report [8] of a hydrothermal preparation of hexagonal ZnS nanowires based on the thermolysis of a novel lamellar covalent organic-inorganic hybrid chalcogenide, ZnS.0.5 EN, in a hot aqueous solution, had been made.

2.2.2 POLYCRYSTALLINE SEMICONDUCTORS

In polycrystalline materials, numerous crystalline regions called grains, have different orientation and are separated by a grain boundary. That is, they have a high degree of order over many atomic or molecular dimensions. These ordered regions or single-crystal regions only vary in size and orientation with respect to one another [50].

These semiconductors can be further classified as (i) microcrystalline and nanocrystalline materials that are usually prepared as thin films and (ii) large grain materials in the form of sliced ingots and sheets. The grain size in polycrystalline materials depends on the substrate temperature during thin film growth, the thickness of the film and also on post-growth annealing treatment of the film. It is important to consider here that many solids are

incorrectly described as being amorphous, but are in fact microcrystalline or nanocrystalline with small crystallite sizes which fail to give crystalline X-ray diffraction patterns. However, often these materials can be confirmed as crystalline using electron diffractions, with lattice images routinely obtained from particles in the range of 5 nm. The grain boundaries generally have an associated space-charge region controlled by the defect structure of the material and the grain boundaries are paths for the rapid diffusion of impurities affecting various properties of polycrystalline materials. An important consequence of the presence of potential barriers on grain boundaries in a polycrystalline semiconductor is the increase of its electrical resistivity. One of the important processes is the decoration of grain boundaries, that is, the process in which precipitates of impurity elements segregate to the boundaries. In general, the grain boundaries introduce allowed levels in the energy gap of a semiconductor and act as efficient recombination centers for the minority carriers. This effect is important in minority-carrier devices, such as photovoltaic solar cells and it is expected that some of the photo generated carriers to be lost through recombination on the grain boundaries. Typically, the efficiency of the device will improve with increasing grain size. In this context, the columnar grain structure (i.e. grains in a polycrystalline material extend across the wafer thickness) is more desirable as compared to the material containing fine grains that do not extend from back to front of a device structure. In order to prevent significant grain boundary recombination of the minority carriers, it is also desirable that the lateral grain sizes in the material be larger than the minority carrier diffusion length. It should also be mentioned that the possible preferential diffusion of dopants along the grain boundaries and or precipitates of impurity elements segregated at the boundaries may provide shunting paths for current flow across the device junction.

It should also be noted that hydrogen passivation of grain boundaries in polycrystalline silicon devices, such as photovoltaic cells, is an effective method of improving their

photovoltaic performance efficiency. This improvement is associated with the mechanism similar to that of the passivation of dangling bonds in amorphous silicon [51].

[55] prepared transparent and polycrystalline zinc sulfide (ZnS) thin film by the chemical bath deposition (CBD) technique onto glass substrates deposited at 80 1C using aqueous solution of zinc acetate, thiourea, triethanolamine and tri-sodium citrate at a pH of about 10.55. Triethanolamine and tri-sodium citrate were used as complexing agents. [56] Had reported ZnS preparation by chemical vapor deposition (CVD) followed by hot isostatic pressing (HIP). The HIP process (uniform compression in a gaseous environment at high temperatures) is known to improve the optical and mechanical properties of polycrystalline zinc sulfide.

2.2.3 AMORPHOUS SEMICONDUCTORS

In contrast to crystalline materials amorphous semiconductors have only short-range order with no periodic structure see **Figure 2.3** These materials can be relatively, inexpensively produced as thin films deposited on large area substrates [50].

An interesting aspect of thin film deposition techniques is that they facilitate the formation of amorphous metal and semiconductor structures relative to bulk preparation methods [17].

What happens to the electron energy band model in a solid without regular crystalline order? The Bloch theorem is not applicable when the structure is not periodic, so that the electron states cannot be described by well-defined *k* values. Thus, the momentum selection rule for optical transitions is relaxed; hence all infrared and Raman modes contribute to the absorption spectra. The optical absorption edge is rather featureless. And since momentum conservation rules or direct and indirect optical transitions no longer apply, in the case of amorphous silicon, e.g., this results in very high absorption coefficient, allowing the use of only micrometer scale thin films for absorption of solar energy. As previously noted, allowed bands and energy gaps still occur because the form of the density of states (DOS) versus energy is determined most strongly by local electron bonding configurations.

In amorphous semiconductors, charge carriers may be scattered strongly by the disordered structure, so that the mean free path may sometimes be of the order of the scale of the disorder. [57] Proposed that the states near the band edges may be localized and do not extend through the solid. It should be noted that the transition from the localized states to the extended states results in a sharp change in the carrier mobility, leading to the presence of the mobility edges or the mobility gap. The carrier mobility in the extended states is higher and the transport process is analogous to that in crystalline materials; whereas in the localized states, the mobility is due to thermally-activated tunneling between those states (i.e., hopping conduction) and it is lower as compared to the extended states. Thus, Anderson localization transition caused by random local field fluctuations due to disorder can lead to "mobility edges" rather than band edges as illustrated in Error! Reference source not found. and hence, ather than an energy gap one has a mobility gap separating localized and non-localized or extended states [16, 51, and 58].

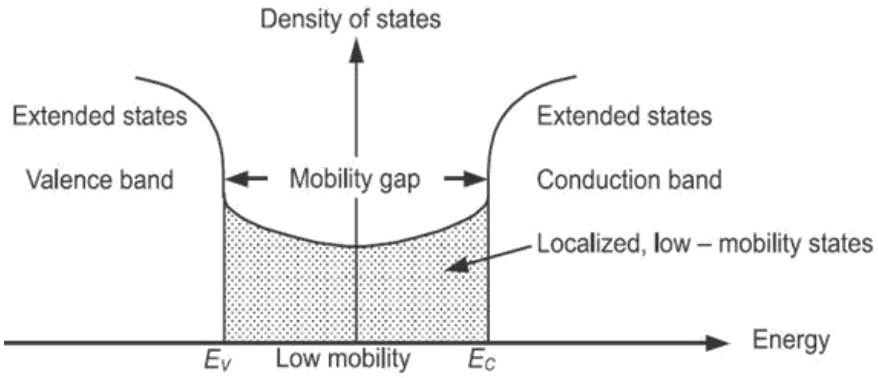

Figure 2.2 Area of mobility between valence and conduction bands

Two distinct classes of amorphous semiconductors are widely studied: tetrahedrally-bonded amorphous solids such as silicon and germanium and chalcogenide glasses. The latter are multicomponent solid of which one major constituent is a "chalcogen" element—sulphur, selenium, or tellurium [58].

The tetrahedrally-bonded materials have properties similar to those of their crystalline forms, provided the dangling bonds defects are compensated with hydrogen. They can be doped with small amount of chemical impurities and their conductivity can be sharply modified by injection of free carriers from a metallic contact. By contrast, the chalcogenide glasses are largely insensitive to chemical impurities and to free carrier injection.

In amorphous materials, defects are of different kind as compared to crystalline materials. In the case of amorphous materials, the main defects are those related to the deviations from the average coordination number, bond length and bond angle; other defects include, e.g., dangling bonds, deviations from an optimal bonding arrangement and micro voids.

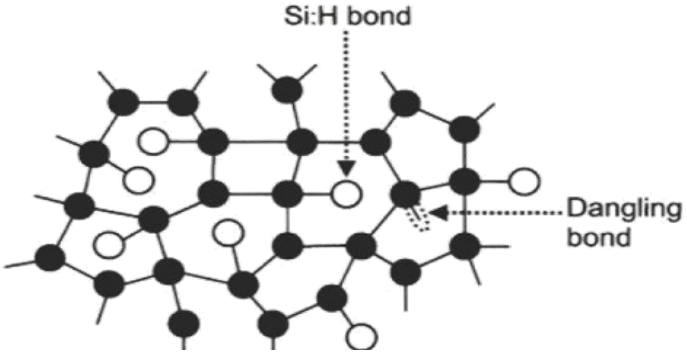

Figure 2.3 Schematic illustration of a two-dimensional continuous random network of atoms having various bonding coordination

As mentioned above, in amorphous semiconductors, the allowed energy bands have band tails in the energy gap [51]. Consider a degenerate direct band gap p-type semiconductor. One can excite electrons from states below the Fermi level, E_f, in the valence band where the band is nearly parabolic, to tail states below conductions band edge, E_c, where the density of states decreases exponentially with energy into the band gap, away from E_c. Such excitations lead to absorption coefficient, α, depending exponentially on photon energy, hv, a dependence that is usually called the Urbach rule, given by

$$\alpha=\alpha_0 \exp [(hv-E_0)/\Delta E]$$

where α_0 and E_0 are material- dependent constants and ΔE, called the Urbach width, is also a material-dependent constant. The Urbach rule was originally reported for alkali halides. It has been observed for many ionic crystals, degenerately doped crystalline semiconductors and

almost all amorphous semiconductors. While exponential band tailing can explain the observed Urbach tail of the absorption coefficient vs. photon energy, it is also possible to attribute the absorption tail behavior to strong internal fields arising, for example, from ionized dopants or defects. Temperature-induced disorder in the crystal is yet another important mechanism that leads to an Urbach exponential absorption tail [14]. The typically observed exponential energy dependence of the absorption edge or the Urbach edge provides an important parameter for characterizing the material's quality and it usually depends on the deposition method and deposition conditions. Thus as already noted above, in amorphous materials the exponential band tails are related to the structural disorder, i.e., bond length and bond angle deviations that broaden the distribution of electronic states; hence, the slope of the Urbach edge can be related to the material's quality [59].

2.3 ZnS FABRICATED BY PHYSICAL METHOD OF FABRICATION

2.3.1 THERMAL EVAPORATION PROCESS

Thermal evaporation is the most common method in producing thin film because the advantages of thermal evaporation are stability, reproducibility, and high-deposition rate. It is well known that the optical parameters of thin-film materials are generally different from those of the same materials in bulk form.

[60] Used acetone- ethanol-cleaned quartz substrates of 2.5-cm diameter. The base vacuum level was maintained at 3.0 ×10-3 Pa, and the deposition pressure was about 5.0×10-3 Pa. The substrates were placed in a rotating holder and kept at a distance of 30 cm from the evaporation source. The rotating substrate- holder helped in obtaining uniformly thick film .They kept electric current for evaporation at 130 A. The nominal film thickness was controlled by an optical thickness monitor. The reference wavelength of optical monitor was 620 nm.

In, [61] the author used ultrasonically cleaned 2–4Ωcm n-type (1 0 0) Si wafers. After that they deposited gold film on the cleaned substrates for about 15 s under 10-1 Torr at 100V and 20mA by using an E 1001 film deposition system. Their synthesis was based on thermal

evaporation of ZnS powders under controlled conditions with the presence of Au films used as catalyst. They performed experiments in a traditional tube furnace system. The ZnS powder was placed at the center of reaction tube and the treated Si substrates were placed next to the ZnS powders and along the downstream side of the flowing argon. Typically, the ZnS source temperature was controlled at about 1293 K. During the growth process of ZnS nanostructures, the 200 sccm Ar and 5 sccm H2 were introduced into the reaction tube and the total pressure was kept at about 150 Torr.

2.3.2 RF MAGNETRON SPUTTERING

Rf magnetron sputtering is one of the cost-effective methods capable of preparing the thin films. This method provides precise structural control at atomic or nonoscale level.

[62] Prepared ZnS film by RF reactive sputtering using Soda Lime glass and Si wafer of 1 in × 1 in as the substrates. Zinc plate was used as the target and mixture of H2S and Ar were used as the reactive gases. All depositions were done at a constant gas pressure of 60 mTorr for 30 min. The chamber was first pumped down to about 1.2×10-6 Torr, and a sputter-etch of 5 min. were done to remove the target surface contamination in each run.

[63] had prepared zinc sulfide (ZnS) target was by taking a suitable aluminum holder (2 in. diameter) and compacting the ZnS polycrystalline powder (99.99%) by applying a suitable hydrostatic pressure (~100 kg/cm2). The fabricated ZnS target was placed in the radio frequency magnetron sputtering (13.56 MHz) chamber for the deposition of nanocrystalline thin films. They used glass and Si as substrates. The glass substrate was cleaned by soap solution, boiling water, ultra sonication, and finally by alcohol vapor for degreasing. The Si wafer was etched by HF (20%) solution for 5 mins. and then sonicated. The chamber was evacuated by to a base pressure of 10-6 mbar. During sputtering, they maintained working pressure ~0.1 mbar by introducing argon as a sputtering gas. For polycrystalline film synthesis by sputtering, in general the sputtering pressure is kept low ~10-3 mbar. But they used comparatively higher pressure (~10-1 mbar) sputtering to increase the scattering probability of the ejected target materials with the plasma neutrals in between the electrodes. Before starting the actual deposition, the target was pre-sputtered and the substrates were

covered by a movable shutter. The sputtering was performed in a RF magnetron sputtering (13.56 MHz) chamber with an effective RF power 170 watt. The target to substrate distance was 3 cm and the substrate temperature was varied from 233 to 273 K.

2.3.3 PULSED LASER DEPOSITION

PLD technique was first used in 1965. This method is currently being used to deposit multi-component ceramic thin films for next generation ceramic devices. PLD deposited metals and alloys at evacuated condition at room temperature shows significant difference in microstructure when compared to conventionally deposited films. This variation is mainly due to the ablated atoms and ions. This method of fabrication is advantageous because it does not require high substrate temperature, as the kinetic energy of the source atoms are sufficient enough to gain mobility. The morphology and stoichiometry of the films can be precisely controlled. It suffers from the drawbacks like nonuniformity of the film and presence of particles on the film surface.

[64] Prepared ZnS thin film by this method on a Si (100) substrate. Prior to deposition, they cleaned the substrate by ultrasonication, methanol, isoporpanol sequentially. They grinded the ZnS powder and then annealed it at 300ºC for 3hrs at base pressure of 10-5 Torr. Then it was cold pressed at 15.5× 108 Pa on 1.27 cm dye. The growth process was carried out in a vacuum chamber with a base pressure of 10-5 Torr. They used a Lambda-Physik EMG 103MSE XeCl LASER with a wavelength of 308 nm for ablation. The LASER pulse energy was kept at 123 mJ with a repetition rate of 10 Hz. Target to substrate distance was kept 3.5 cm.

[65] Used a KrF excimer laser operating at 248 nm. The laser beam of energy density 8.8 J/cm2 with a repetition rate of 5 Hz was used to ablate from the sintered ZnS target. Before deposition, the chamber was pumped down to a base pressure of 1.0 ×10-5 Torr. The distance between the target and substrate was maintained at 4 cm. During deposition, argon gas with a flow rate of 20 cm was fed through the mass flow controller into the chamber, and a working pressure of 0.1 Torr was maintained. The deposition time of ZnS thin films is 60 min.

2.3.4 CLOSED SPACE EVAPORATION (CSE)

This is a low cost and non-wet technique that has good control over the rate of deposition. The loss of material could be reduced during the film growth in this technique. As a result of the high kinetic energy of the vapors, highly adherent and uniform layers can be achieved. *Y.P. Venkata Subbaiah et al*. used ultrasonically cleaned Corning 7059 glass slides as substrates for depositing ZnS films. 5N pure ZnS powder, procured from *Koch Chemicals Ltd.*, England was used to produce the layers. The films were deposited at different substrate temperatures that vary in the range, 200– 350 ºC.

2.4 ZnS FABRICATED BY CHEMICAL METHOD OF FABRICATION

2.4.1 SPRAY PYROLYSIS

Spray pyrolysis is basically a chemical deposition technique in which fine droplets of the desired material solution are sprayed onto a heated substrate. The atomizer, which is the main part, consists of a nozzle mounted in a 100 ml glass round-bottom flask. The deposition of II-VI semiconductors by the spray pyrolysis technique was first investigated by [66]. Spray Pyrolysis technique of preparation of thin films is very attractive because it is inexpensive, simple and capable of depositing optically smooth, uniform and homogeneous layers. It is also is one of the most cost effective and scalable chemical techniques for fabrication of ZnS thin film.[67] had reported ZnS thin films were deposition by using two different precursors for zinc- zinc acetate and zinc chloride, and thiourea was chosen as the precursor for sulphur. The respective precursor solutions were mixed together and stirred well for homogeneity. 50 ml of precursor solution was sprayed at a spray rate of 5 ml/min onto soda lime glass substrates maintained 450ºC.

[68] Used zinc chloride solution at 0.07M concentration and 0.07M thiourea ($SC(NH_2)_2$) solution in deionized water. The prepared solution is sprayed at different spray rates (1.5–6 ml min^{-1}) onto the clean glass substrates, heated from 300 to 500ºC.Compressed air was used as carrier gas.

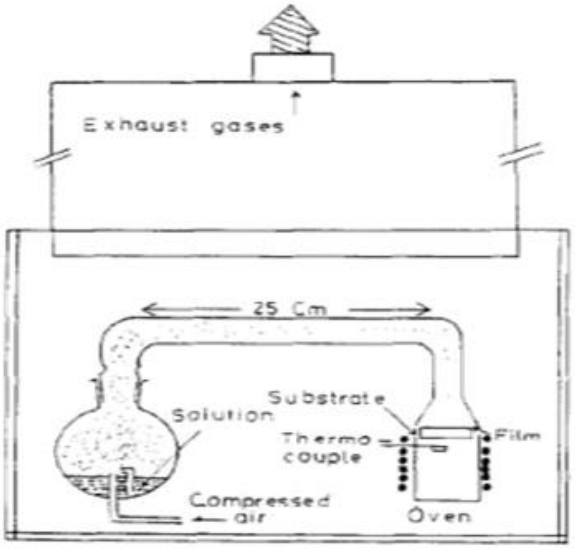

Figure 2.4 Schematic diagram of Spray Pyrolysis apparatus

2.4.2 CHEMICAL VAPOUR DEPOSITION (CVD)

Chemical vapor deposition (CVD) has grown very rapidly in the last four decades and applications of this fabrication process are now key elements in many industrial products, such as semiconductors, optoelectronics, optics, cutting tools, refractory fibers, filters and many others. CVD can also be used to produce fibers, monoliths, foams and powders. CVD is economically competitive also. The deposition rate is high and thick coatings can be readily obtained.

In [69], the author prepared monolithic ZnS by the CVD reaction between zinc and hydrogen sulfide at elevated temperatures of 650–750 ◦C and low pressures of around 50 mbar. The zinc to H2S molar ratio was adjusted close to 1.0 and the deposition rate of 80–100μm/h was achieved by controlling the reactant fluxes. The samples were grown on graphite substrates in the form of flat plates.

In [70], the author made zinc sulfide (ZnS) thin films (thickness ~150–170 nm) on silicon (100) substrates by single source chemical vapor deposition (SS-CVD) using zinc di-ethyl-di-thio-carbamate ($Zn[S_2CN(C_2H_5)_2]_2$) as the precursor. A maximum crystallite size of ~50 nm was obtained at 400°C. Rather than using two different materials as zinc and sulphur (eg. H2S and dimethyl/diethylzinc) source, he employed a material which contains both of them.

The deposition of the film was effected by vaporizing the single source substrate in vacuum and decomposition of the vapor on the heated substrate.

$$Zn[S_2CN(C_2H_5)_2]_2 \xrightarrow{400-500^{\circ}C} ZnS + C_2H_5NCS + (C_2H_5)_2NH + CS_2 + C_2H_4$$

In, [71] the author reported high vacuum chamber with a background pressure of~ 2 x10-7 Torr. The precursor partial pressure was at ~2 x10-5 Torr and growth temperatures ranged from 300°C to 500°C The TEM micrographs indicated that the film was densely packed with columnar structures perpendicular to the substrate surface (diameter of the columns was ~0.2–0.4 mm). Electron diffraction indicated that the films were cubic (Sphalerite). The intense diffraction peak (2u _28.78) in the film grown at 450 °C was due to the reflection of ZnS cubic (1 1 1) plane. The presence of the single peak indicated that the crystallites within columns had preferred orientation along [1 1 1] direction. The film grown at 300°C showed no diffraction peaks and was considered amorphous. The carbon concentration at the film surface (~26 at%) was predominantly adventitious hydrocarbons, virtually removed after the Ar+ etching procedure with subsequent carbonaceous impurity remaining below ~1 atomic percent throughout the film. [72] deposited ZnS in a low ambient atmosphere of hydrogen sulfide (H_2S ~10^{-4} Torr). The H_2S atmosphere was obtained by a controlled thermal decomposition of thiourea [$CS(NH_2)_2$] inside the vacuum chamber. It had been observed that at elevated substrates temperature of about 200 °C helps eject any sulfur atoms deposited due to thermal decomposition of ZnS during evaporation. The zinc ions promptly recombine with H_2S to give better stoichiometry of the deposited films. The thermal decomposition of thiourea [$CS(NH_2)_2$] is a convenient source of H_2S, which was controlled by regulating the temperature of the electrically heated test tube inside the evaporation chamber. The higher reactivity of H2S has ensured a better conversion of the dissociated zinc ions into ZnS and also has not produce any excess of sulfur at the substrate. Furthermore, keeping the substrate at an elevated temperature has ejected the dissociated sulfur ions deposited during growth. ZnS powder was evaporated using a molybdenum boat filament in a high vacuum chamber

(pressure ~5 x 10^{-5} Torr). During the deposition of ZnS films, the filament and substrate were kept about 10 cm apart for formation of quite uniform films. The films were deposited on the glass substrates held at 200ºC in a vacuum (~5 x 10^{-4} Torr). In all samples, the deposition time of 20 min was the maximum time duration for obtaining a film thickness in 400–500 nm in normal and H_2S ambient.

2.4.3 SUCCESSIVE IONIC LAYER ADSORPTION AND REACTION (SILAR) METHOD

The SILAR technique, introduced by [73] is a unique method in which thin films of compound semiconductors can be deposited by alternate dipping of a substrate into the aqueous solutions containing ions of each component. The SILAR method resembles CBD but deposition control of the growth is easier since the precursors for the cation and anion constituents of the thin film are in different vessels. The growth of thin films in the SILAR method occurs only heterogeneously on the solid–solution interface due to the intermediate rinsing step between the cation and anion immersions. Therefore, the thickness of the film can be controlled simply by the number of growth cycles. The equipment for the SILAR technique can be very simple and inexpensive due to the ambient growth conditions used.

[74] deposited ZnS on well cleansed glass substrate. They immersed a well-cleaned glass substrate is in the first reaction vessel containing aqueous cation precursor 0.1M ZnCl2 solution at pH 5.5. After the cation immersion, they moved the substrate to the rinsing vessel where it was washed with purified water. The sulfide ions were adsorbed from an aqueous 0.05 M Na2S solution with pH 12. After anion immersion, the substrate was washed; thus the first SILAR growth cycle was finished. Repeating these cycles a thin film with desired thickness was grown. They obtained a ZnS film of 90nm thickness by repeating such SILAR cycles 40 times. The cation and anion immersion times were 20 s and the rinsing time was 100 s. The temperature of the solutions was maintained at 27ºC (± 1ºC).

2.4.4 SOL-GEL

Sol–gel process is one of the most commonly used techniques in thin film deposition. Sol–gel process is particularly attractive because it is a solution-based process, offers high material utilization and much higher deposition rate.

It provides film thickness control at the Angstrom level, and therefore allows one to tune the band gap and related properties through control of particle size.

In [75], the author films on Corning Eagle 2000 glass substrates by sol– gel deposition technique. He used Zinc acetate 99.999%, aqua ammonia (30%), isopropanol (IPA) and thiourea (99.0%). He mixed equimolar of 0.7 M zinc acetate and thiourea in IPA and aqua ammonia. Weight of zinc acetate and thiourea were varied to get different stoichiometry. The chemical compounds were magnetically mixed for over 2 hrs at 80ºC and left to age for at least a day to form the sol. Corning glass substrates were sequentially cleaned in acetone, IPA and water respectively, and blow dry with N2. The derived sols were spin onto a pre-cleaned Corning glass substrate at spinning speed of 3000rpm. The deposition cycle was repeated until a thickness of 250nm was obtained. Each coating was dried using a hotplate through two stage heat treatments at250ºC to move the solvents and at400ºC, 450ºC, 500ºC and 550ºC for1hr to sinter the films.

In [76], the authors deposited ZnS film on polished (100) Si wafers. Zinc acetate dihydrate, $Zn(OAc)_2 \cdot 2H_2O$, manganese acetate tetrahydrate, $Mn(OAc)_2 \cdot 4H_2O$, sodium sulfide nonahydrate, $Na_2S \cdot 9H_2O$ were used by them. Si wafers were sonicated in CCl_4 for 15 min and then rinsed with isopropanol and water. OH-terminated Si surfaces (Si-OH) were prepared by 30 min sonication in 'piranha' solution (4:1 conc. H_2SO_4:30%H_2O_2) and rinsed with abundant amount of water. Si-OH substrate was then immersed (for 5 min) in an aqueous solution of $Zn(OAc)_2$ (91 mM). Then the substrate was rinsed with water and dried in a stream of Ar. The substrate then was immersed in aqueous Na2S solution (4 mM) for 2 min, rinsed with water and dried in Air. By repeating these two-step adsorption cycles, multilayer film was synthesised.

2.4.5 CHEMICAL BATH DEPOSITION (CBD)

CBD method is most commonly used because it is a very simple, cost effective and economically reproducible technique that can be applied in large area deposition at low temperature. This is a low cost and non-wet technique that has good control over the rate of deposition. This technique is based on the controlled release of metal ion (M^{2+}) and sulfide (S^{2-}) in an aqueous bath in which the substrates are immersed. In this process, release of metal ion (M^{2+}) is controlled by using a suitable complexing agent (A chelating agent, used to limit the hydrolysis of the metal ion and bring some stability to the bath, which would otherwise undergo rapid hydrolysis and precipitation). The deposition begins with nucleation phase followed by growth phase in which the thickness of film increases with duration up to the terminal phase where film depletion into constituent ions occurs after a certain time.

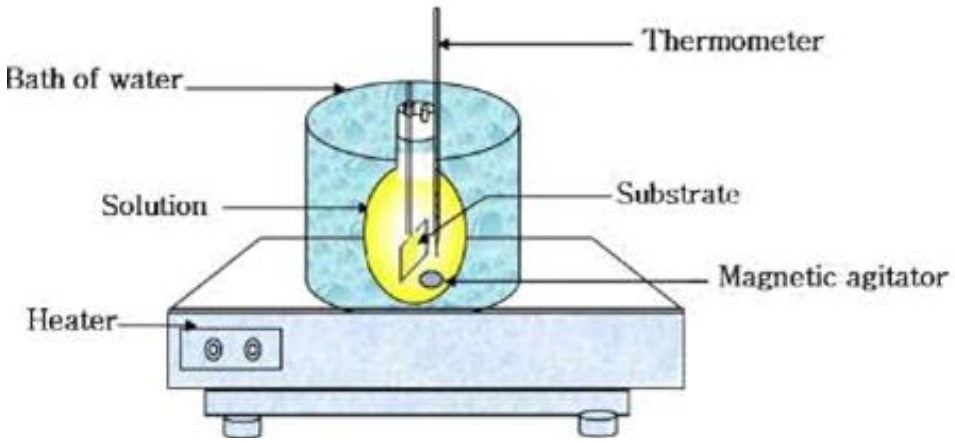

Figure 2.5 CBD System

[77] used aqueous solutions of 0.045 M zinc acetate dehydrate ($Zn(CH_3COO)_2 \cdot 2H_2O$), 0.065Mthiourea ($H_2NCSNH_2$), 0.133M tartaric acid ($COOH(CHOH)_2COOH$) as a complexing agent and 80% hydrazine hydrate for ZnS thin film deposition. They mixed 10 ml zinc acetate solution and 10 ml tartaric acid solution and stirred for several minutes to get a clear and homogeneous solution. Thereafter, 5ml of 80% hydrazine hydrate was added followed by the addition of 10 ml thiourea solution under stirring condition. Finally 0.4 ml

ammonia (13.4 N) was added to make the solution alkaline and the pH was maintained at ≈10. A glass substrate was then placed vertically inside this beaker without disturbing it. The beaker was sealed with a Teflon tape. The whole solution was kept in an oil bath maintaining the temperature at 85 °C for 3 h. After completion of film deposition, the glass slide was removed from the beaker and was cleaned with de-ionized water ultrasonically to remove the white, loosely adherent powders precipitates in the solution during deposition. A very thin, uniform colorless film with the thickness of 110 nm was obtained having good adherent property.

[78] prepared ZnS thin films from solution containing 2.5×10−2 M of zinc sulphate ($ZnSO_4$), 3.5×10−2 M of thiourea ($SC(NH_2)_2$, 1M ammonia (NH_4OH) and 3M of hydrazine hydrate (N_2H_4, H_2O). ZnS films were also prepared by them using a solution containing 7.7×10−2M of zinc chloride ($ZnCl_2$), 7.1×10−2 M of thiourea, 1.39M of ammonia and 2.29M of hydrazine hydrate.

2.4.6. PHOTOCHEMICAL DEPOSITION (PCD)

To reduce the manufacturing cost for solar cells, researchers have been attempting to prepare compound semiconductors by photochemical deposition (PCD), which is a technique of film preparation by UV light illumination to a substrate immersed in a deposition solution. Ions in the solution are excited by the UV light, and chemical reactions are thus induced. PCD is an economical and simple technique and enables large-scale deposition. Moreover, the deposition reactions are easily controlled by turning on/off the light. The reaction in PCD is mainly controlled by bath temperature.

[79] used an indium–tin-oxide (ITO)-coated glass sheet was as a substrate. Aqueous solutions containing 1 m mol/l $ZnSO_4$, 600 m mol/l $Na_2S_2O_3$, and a small amount of H_2SO_4 (for adjusting pH to 3.5) was used by them. They immersed the degreased substrate at about 3 mm below the solution surface and illuminated it by an ultrahigh-pressure mercury arc lamp of 500 W through a spherical simple lens. The diameter of the illuminated region was about 10 mm. The growth solution was stirred during the deposition. The $Na_2S_2O_3$ concentration was increased to prevent deposition of metallic Zn.

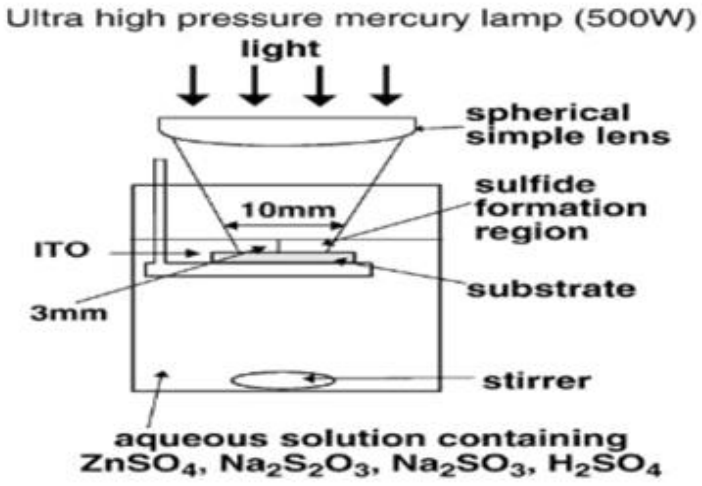

Figure 2.6 Schematic Diagram of PCD set up

[80] had reported the formation of ZnS thin film by using PCD technique and they also presented a study related to the effect of different factors like pH of the solution and stirring speed of the solution on the growth of the film.

2.4.7 ATOMIC LAYER EPITAXY (ALE)

Atomic Layer Epitaxy (ALE) or Atomic Layer Deposition(ALD) growth is based on deposition technique in which the reactants are supplied alternately to the substrate and where the saturated surface reactions result in the growth of a full or a partial monolayer of the material to be formed. It is a self-limiting reaction and it allows the precise control of film thickness with high spatial uniformity and low pin-hole density. This deposition technique was first demonstrated by [81] for the growth of polycrystalline ZnS and for dielectric oxides such as Al_2O_3. ALD was developed originally for the fabrication of Thin-film Electroluminescent (TFEL) displays.

In, [82] the author reported the deposition of polycrystalline ZnS thin film using the precursors of diethyl zinc (DEZ) and H2S in the substrate temperature range of 250–400ºC. They used a travelling-wave-type ALD reactor *(F-450, Microchemistry Ltd.)* having the large plates of dimension 16 in×12 in. for holding sample. Firstly, amorphous Al_2O_3 films of thickness 100 nm were deposited by ALD using the precursors of trimethyl aluminum and water. One cycle of the ALD process consisted of 0.6 s DEZ pulsing, 2.2 s purging, 1.0 s H_2S

pulsing, and 3.3 s purging. Nitrogen was used as a carrier and purging gas. The reactor pressure during a process was under 10 mbar.

Gert Stuyven et al. examined the ZnS ALD growth based on DEZn and H_2S in the temperature range of 200–350ºC [36]. The growth rate was shown to be strongly influenced both by the purge times and by the DEZn dosing, which gave a strong indication that the surface stability after the DEZn precursor pulse is the limiting factor for ALD growth.

2.5 OPTICAL PROPERTIES AND BAND GAP

Optical properties of semiconductors typically consist of their refractive index *n* and extinction coefficient *k* or absorption coefficient α (or equivalently the real and imaginary parts of the relative permittivity) and their dispersion relations, that is their dependence on the wavelength, λ, of the electromagnetic radiation or photon energy *hv*, and the changes in the dispersion relations with temperature, pressure, alloying, impurities, etc. A typical relationship between the absorption coefficient and photon energy observed in a crystalline semiconductor is shown in **Figure 2.4,** where various possible absorption processes are illustrated 14]. The important features in the α vs. *hv* behavior as the photon energy increases can be classified in the following types of absorptions: (a) Reststrahlen or lattice absorption in which the radiation is absorbed by vibrations of the crystal ions, (b) free-carrier absorption due to the presence of free electrons and holes, an effect that decreases with increasing photon energy, (c) an impurity absorption band (usually narrow) due the various dopants, (d) exciton absorption peaks that are usually observed at low temperatures and are close to the fundamental absorption edge and (e) band-to-band or fundamental absorption of photons, which excites an electron from the valence to the conduction band [14].

The absorption coefficient due to the inter-band transition is usually very large. However, the absorption coefficient becomes very small (<1 cm^{-1}) when the photon energies fall below the band gap energy. In this case, another type of optical absorption process takes place which results in electronic transitions only within the allowed energy band and is called the free-carrier absorption process. This type of absorption result in the excitation of lattice phonons, accelerate free electrons in the conduction band or creation of an excitation [7].

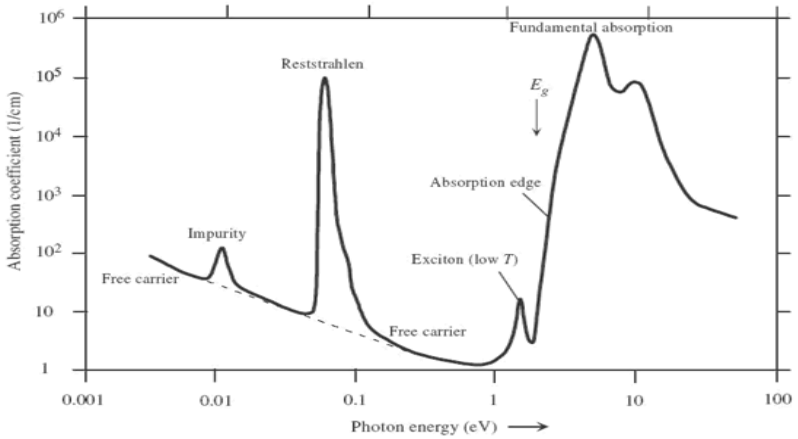

Figure 2.7 Absorption coefficient is plotted as a function of the photon energy in typical semiconductor to illustrate possible absorption processes

In order to understand the optical behavior of films, one must become familiar with the optical constants of materials, their origins; magnitudes and how they depend on the way films are processed. The unifying concept that embraces all optical properties is the interaction of electromagnetic radiation with the electrons of the material. On this basis, optical properties are interpretable from what we know of the electronic structure and how it is affected by atomic structure, bonding, impurities, and defects [17].

The optical transmission is over 80% in the visible region. The values of absorption coefficient are calculated by using this equation:

$$I_1 = I_0 \exp(-\alpha t)$$

Where α is the optical absorption coefficient, t is the thickness of the film, I_1 and I_0 are the intensity of transmitted light and initial light respectively.

The absorption coefficient (α) is related to the incident photon energy as:

$$\alpha = k(h\upsilon - E_g)^{n/2} / \upsilon$$

Where K is constant, Eg is the energy gap and n is constant equal to 1 for direct gap compound. The variation of (αhν)2 versus (hν) is plotted. The direct band gap values are

measured by extrapolating the straight-line portion over the hυ-axis. The band gap value (Eg) calculated from this linear-fit plot is about 3.69 eV, which is well matched with the band gap value (3.68 eV) for the bulk ZnS [30].

2.6 ZINC SULFIDE BASED SOLAR CELLS

Several works on solar cell using ZnS- buffer layer has been reported. Most of those studies concentrated on CIGS-ZnS cells.[83] reported on recent enhancements to device performance leading to a certified total-area energy conversion efficiency of 18.6% for Cu(In,Ga)Se2 solar cells that incorporate a ZnS(O,OH) buffer layer as an alternative to CdS.

In [84], it has been reported that the MBE-grown polycrystalline CIGS on a molybdenum coated SLG substrate over which ZnS was grown in a a separate MBE process. The result of their study is given below,

Table 2.1 CIGS Solar Cell Performance with MBE-ZnS buffter layer

Sample	Sub-temp. (°C)	Eff. (%)	J_{sc} (mA/cm^2)	V_{oc} (V)	FF
1	RT	0.12	3.23	0.18	0.32
2	150	2.47	24.3	0.25	0.41
3	195	4.12	30.5	0.26	0.52
4	200	5.34	28.6	0.37	0.50
Ref. (CdS buffer)		15.3	30.9	0.69	0.72

2.7 APPLICATION OF ZNS FOR THE FABRICATION OF OTHER OPTOELECTRONIC DEVICES

- UV light emitting diodes
- Blue light emitting diodes
- Emissive flat screen
- Antireflection coating in solar cell technology

- Alpha particle detectors
- Thin film electroluminescent devices(TFEL)
- LED
- CRT screen
- Field emitters
- Field effect transistors (FETs)
- p-type conductors
- Gas sensors
- Chemical sensors
- Biosensors
- Nano-generators

3. CHAPTER THREE

3.0 EXPERIMENTAL DETAILS

3.1 SURFACE PREPARATION OF SUBSTRATES

A clean surface is one that contains no significant amount of undesirable material [85]. Cleaning is defined as the removal, by physical and or chemical means, of soil that could interfere with the preparation of the desired material. Soil is matter on the surface whose chemical characteristics are different from those being formed. The types of soils most commonly encountered are fingerprint oils, metal oxides, dirt, etc. [4] the nature and surface finish of the substrates are extremely important because they greatly influence the properties of films deposited on them [6]. It is therefore important that prior to the deposition of the semiconducting thin film the substrate, in this case, microscope glass slide is cleaned thoroughly to remove any undesirable substance from it.

Soda-lime glass slides were used as substrates for deposition of ZnS thin films. Before deposition, the substrates were ultrasonically cleaned sequentially in acetone, ethanol, and deionized water for 15 min each and rinsed with deionized water between each step. Clean substrates were finally dried in air.

3.2 REAGENTS

The chemicals used for the film preparation are listed as follows:

- zinc sulfate ($ZnSO_4$ $7H_2O$)
- thiourea [$SC(NH_2)_2$]
- ammonia (NH_3)
- and hydrazine hydrate (N_2H_4)

3.2.1PREPARATION OF 0.1M ZINC SULFATE ($ZnSO_4$ $7H_2O$)

2.87 g of zinc sulfate ($ZnSO_4$ $7H_2O$) was weighed into a beaker. The salt was dissolved into 90 ml distilled water under continuous stirring to produce 0.1M zinc sulfate ($ZnSO_4$ $7H_2O$).

3.2.2 PREPARATION OF 0.67 M AND 0.83 M THIOUREA [$SC(NH_2)_2$]

4.57 g and 5.7 g thiourea [$SC(NH_2)_2$] were mixed with reaction solution containing 90 ml distilled water into 150 ml beaker under continuous stirring to produce 0.67 M and 0.83 M thiourea [$SC(NH_2)_2$] respectively.

3.2.3 PREPARATION OF 0.74 M, 1.48 M AND 2.97 M AMMONIA (NH_3)

5 ml, 10 ml and 20 ml ammonia (NH_3) were mixed with reaction solution containing 90 ml distilled water into 150 ml beaker under continuous stirring to produce 0.74 M, 1.48 M an2.97 M thiourea [$SC(NH_2)_2$] respectively.

3.3 PREPARATION OF THE THIN FILM

ZnS thin films were deposited onto the substrates by CBD using zinc sulfate, hydrazine hydrate, ammonia, thiourea powder and deionized water as precursor materials.

In a typical synthesis process, 100 ml of reaction solution was obtained by mixing 20 ml of 0.5 M zinc sulfate, 5 ml of 80% hydrazine hydrate, 5 ml of 25% ammonia, 5.70 g of thiourea powder and 70 ml of deionized water. First, zinc sulfate solution was mixed with hydrazine hydrate and ammonia in a 100-ml beaker under continuous stirring. Initially, the solution was milky and turbid due to formation of $Zn(OH)_2$ in suspension. The solution became clearer with stirring. Then deionized water and thiourea powder were added to the solution and the mixture was stirred under ambient conditions for 5 min. The pre-cleaned substrates were vertically immersed into the reaction solution. The beaker was sealed to prevent evaporation. CBD was performed at a temperature of 70 °C for 2 h in the bath. After deposition, the substrates were removed from the solution and rinsed in deionized water to remove loosely adherent ZnS particles from the surfaces before they were dried in air.

To study the effect of thiourea and ammonia concentrations on the properties of ZnS thin films, two sample series were prepared by varying the thiourea concentration or the ammonia concentration separately while keeping the other reagent concentrations constant. The deposition parameters for different samples are listed in Table 1.

The samples obtained were characterized by means of X-ray diffraction (XRD), scanning electron microscopy (SEM), energy-dispersive spectroscopy (EDS) and UV-visible spectroscopy (UV/Vis spectrometer). XRD patterns were obtained using a Cu K_α radiation source ($\lambda = 0.1542$ nm) over diffraction angles ranging from 20° to 80° at a scanning speed of 6° min^{-1} with a grazing angle of 0.5°. Optical transmission measurements were performed using a UV-Vis spectrometer at room temperature in the wavelength range from 300 to 1100 nm.

3.3.1 REACTION MECHANISM

The deposition process is based on the slow release of Zn^{2+} and S^{2-} ions in solution which then condense on the substrate. The deposition of ZnS occurs when the ionic product of Zn^{2+} and S^{2-} exceeds the solubility product of ZnS. $ZnSO_4$ is used as the Zn^{2+} source and thiourea supplies S^{2-} ions through hydrolysis according to the following equations:

$$ZnSO_4 = Zn^{2+} + SO_4^{2-} \quad (1)$$

$$SC(NH_2)_2 + OH^- = SH^- + CH_2N_2 + H_2O \quad (2)$$

$$SH^- + OH^- = S^{2-} + H_2O \quad (3)$$

The first complexing agent is NH_3, which hydrolyses in water to give OH^- according to:

$$NH_3 + H_2O = NH_4^+ + OH^- \quad (4)$$

The second complexing agent is N_2H_4, which also hydrolyses in water to give OH^- according to:

$$N_2H_4 + H_2O = N_2H_5^+ + OH^- \quad (5)$$

Zn^{2+} ions form the metal complexes with ammonia and hydrazine hydrate by the following reactions:

$$Zn^{2+} + 4NH_3 = [Zn(NH_3)_4]^{2+} \quad (6)$$

$$Zn^{2+} + 3N_2H_4 = [Zn(N_2H_4)_3]^{2+} \quad (7)$$

From equations (3), (6) and (7) complexes and sulfide ions migrate to the substrate surface, where they react to form ZnS:

$$Zn(NH_3)_4^{2+} + S^{2-} = ZnS + 4NH_3 \quad (8)$$

$$Zn(N_2H_4)_3^{2+} + S^{2-} = ZnS + 3N_2H_4 \quad (9)$$

Assuming the metallic complex of the form $ZnLn^{2+}$, where L is the complexing agent, the general reaction for the ZnS deposition can be represented as:

$$ZnLn^{2+} + CS(NH_2)_2 + 2OH^- \rightarrow ZnS(substrate) + nL + 2NH_3 + CH_2N_2 + 2H_2O \quad (10)$$

During the deposition of ZnS thin films, according to the reactions (4) and (5), the formation of $Zn(OH)_2$ occurs as a competitive process in the bath. So we can expect that the Zn^{2+} ions have to be in form of $Zn(OH)_2$ precipitate, however it is not true due to the presence of NH_3 which forms with Zn^{2+}, the complex $Zn(NH_3)_4^{2+}$ which is soluble in this medium[1 1].

O'Brien and McAleese proposed two possible reaction mechanisms for the growth of ZnS films [40]. The first is a cluster-by-cluster process, in which colloidal ZnS particles preformed in solution via homogeneous reaction agglomerate and then adsorb on the surface to form a film. Hence, the film consists of larger spherical particles and exhibits poor compactness and adherence. The second is an ion-by-ion process, in which ions condense on the reacting surface to form a film via a heterogeneous reaction. Hence, the film consists of very small particles with excellent compactness and adherence. Ion-by-ion growth involves heterogeneous nucleation on the substrate surface and subsequent growth of nuclei.

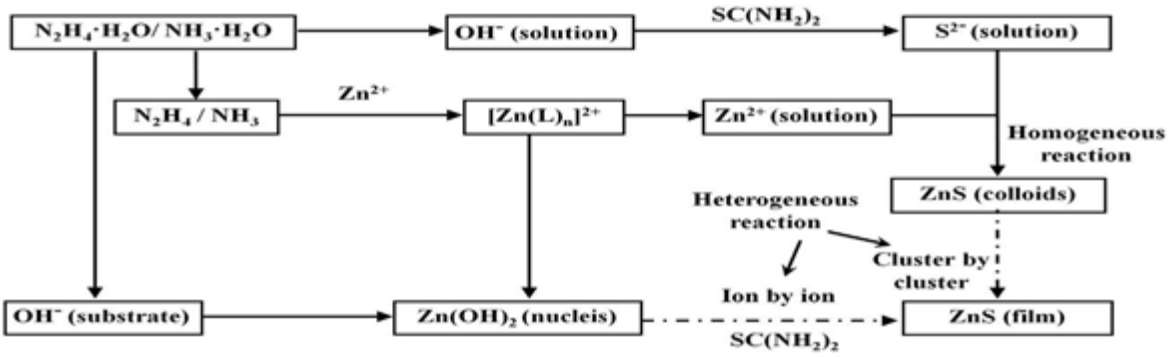

Figure 3.1 Growth mechanism for ZnS thin films in aqueous alkaline solution

In general, OH^- first adsorbs onto the substrate and then water-soluble $[Zn(L)_n]^{2+}$ complex ions react with OH^- to release Zn^{2+} and form $Zn(OH)_2$, which serves as nuclei on which thiourea is adsorbed and hydrolyzed to form a ZnS film. In fact, a mixed mechanism is typically involved in the growth of ZnS films in **Figure 3.1**, it is critical to restrain the cluster-by-cluster mechanism and encourage the ion-by-ion process for the formation of high-quality ZnS films. The process depends on suitable deposition parameters, such as the bath temperature, pH of the reaction solution and the concentration of the reacting species.

Table 3.1 Deposition parameters for various samples

Sample	Concentration (M)				Temperature (°C)	Deposition Time (min)
	$ZnSO_4$	$N_2H_4.H_2O$	$NH_3.H_2O$	$SC(NH_2)_2$		
a_1	0.1	0.82	0.74	0.83	70	120
a_2	0.1	0.82	1.48	0.83	70	120
a_3	0.1	0.82	2.97	0.83	70	120
b_1	0.1	0.82	0.74	0.67	70	120
b_2	0.1	0.82	0.74	0.67	70	120

4. CHAPTER FOUR

4.0 CHARACTERIZATION OF ZnS THIN FILMS

4.1 STRUCTURAL AND MORPHOLOGICAL PROPERTY STUDIES

In this category of study, the X-ray diffraction pattern, surface morphology and compositional ratio of the constituent elements in the deposited film have been mainly analyzed. The particle grains structure, uniformity of the surface morphology, crystallinity, and grain boundary are some of the important attributes and parameters on which the studies are mainly focused to determine the structural behavior for the fabricated thin films.

4.1.1 X-RAY DIFFRACTION (XRD)

X-ray Diffraction is a tool used for determining the atomic and molecular structure of a crystal, in which the crystalline atoms cause a beam of incident X-rays to diffract into many specific directions. By measuring the angles and intensities of these diffracted beams, a crystallographer can produce a three-dimensional picture of the density of electrons within the crystal. In an X-ray diffraction measurement, a crystal is mounted on a goniometer and gradually rotated while being bombarded with X-rays, producing a diffraction pattern of regularly spaced spots known as reflections. The incoming beam (coming from upper left) causes each scatterer to re-radiate a small portion of its intensity as a spherical wave. If scatterers are arranged symmetrically with a separation d, these spherical waves will be in sync (add constructively) only in directions where their path-length difference 2d sin θ equals an integer multiple of the wavelength λ. i.e. $n\lambda = 2d\sin\theta$.

In that case, part of the incoming beam is deflected by an angle 2θ, producing a *reflection* spot in the pattern. Here d is the spacing between diffracting planes, θ is the incident angle, *n* is any integer, and λ is the wavelength of the beam.

XRD is a non-destructive technique which is mainly used for measuring the average spacing between layers or rows of atoms, determining the orientation of a single crystal or grain,

finding the crystal structure of an unknown material and measuring the size, shape and internal stress of small crystalline regions.

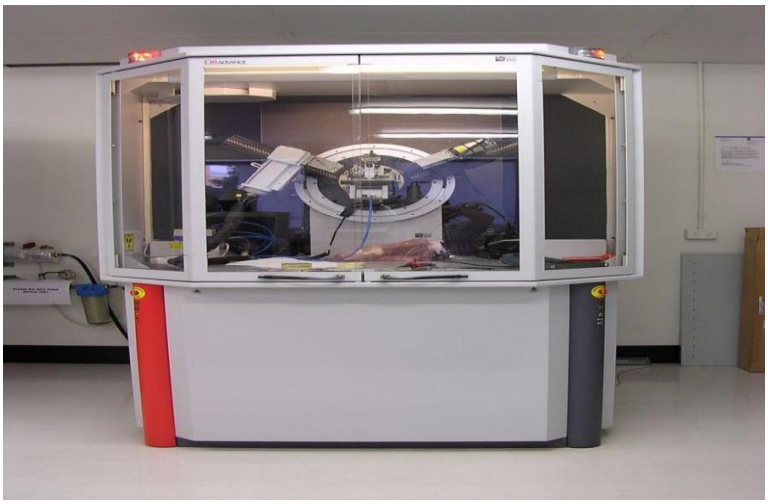

Figure 4.1 XRD Machine

4.1.2. SCANNING ELECTRON MICROSCOPY (SEM)

A scanning electron microscope (SEM) is a type of electron microscope. It uses a focused beam of high-energy electrons to generate a variety of signals at the surface of solid specimens. The signals that derive from electron-sample interactions reveal information about the sample including external morphology (texture), chemical composition, and crystalline structure and orientation of materials making up the sample. . SEM analysis is considered to be "non-destructive"; that is, x-rays generated by electron interactions do not lead to volume loss of the sample, so it is possible to analyze the same materials repeatedly.

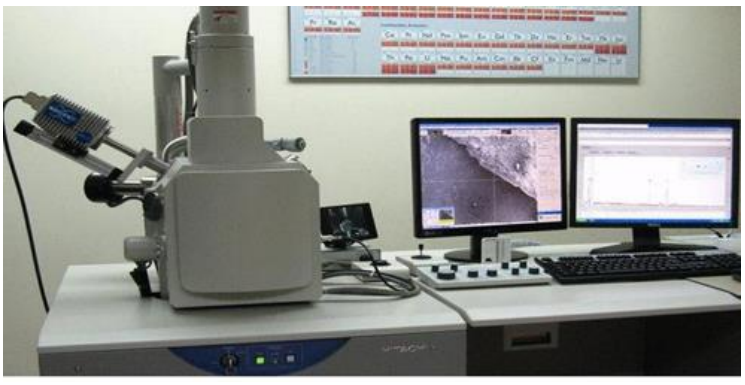

Figure 4.2 SEM Machine

Energy Dispersive X-ray (EDX) Energy-dispersive X-ray spectroscopy (EDS, EDX, or XEDS), sometimes called energy dispersive X-ray analysis (EDXA) or energy dispersive X-ray microanalysis (EDXMA), is an analytical technique used for the elemental analysis or chemical characterization of a sample. EDS makes use of the X-ray spectrum emitted by a

solid sample bombarded with a focused beam of electrons to obtain a localized chemical analysis [40]. The number and energy of the X-rays emitted from a specimen can be measured by an energy-dispersive spectrometer. As the energy of the X-rays is characteristic of the difference in energy between the two shells, and of the atomic structure of the element from which they were emitted, this allows the elemental composition of the specimen to be measured.

Three broad categories are used when referring to the concentrations of elements present in a sample:

1. Major Components - More than 10 wt %;
2. Minor Components - 1-10 wt %;
3. Trace Elements - Less than 1 wt %.

4.2 OPTICAL PROPERTY STUDIES

The optical property study forms a considerable part while evaluating a cell performance or that of a thin film. The photo absorption transmission characteristics, direct and indirect band-gap evaluation are some of the important parameters that are determined to characterize a thin film. However, in this work, the focus has been mostly concentrated on ascertaining the band-gap for the electrodeposited ZnS thin films using the UV transmission spectroscopy.

4.2.1 UV- VISIBLE SPECTROSCOPY

Spectroscopy is the terms used to refer to the measurement of radiation intensity as a function of wavelength and are often used to describe experimental spectroscopic methods. Spectral measurement devices are referred to as spectrometers. In my present work Spectrometer was used to measure the transmissivity (%) and reflectance (%) of the prepared samples.

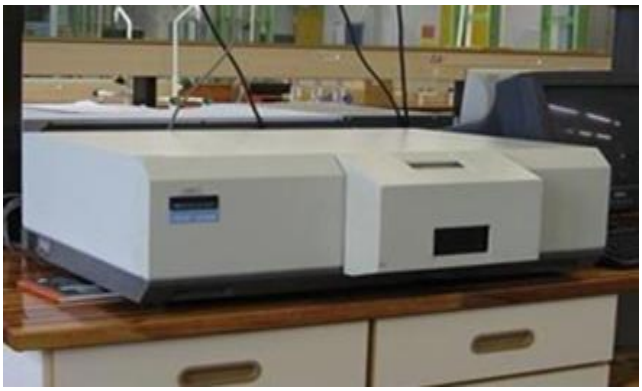

Figure 4.3 Spectrophotometer

5. CHAPTER FIVE

5.0 RESULTS AND DISCUSSION

5.1 X-RAY DIFFRACTION STUDIES

ZnS can exist in a cubic (zinc-blende type) or hexagonal (wurtzite) structure. Oladeji and Chow reported that chemically deposited ZnS thin films are highly disordered materials but can be transformed into a wurtzite-2H phase by annealing [38]. Göde et al. obtained an amorphous film at 60–70 °C and a wurtzite-2H phase at 80 °C [86]. Fig. 5.1 shows XRD patterns for ZnS films after multiple depositions for 2h. Multiple depositions were carried out by placing the substrate into fresh solution and allowing growth to proceed for 2 h, and this process was repeated three times. . In several studies, very thin ZnS films showed no discernible XRD peaks [33, 87 and 88]. XRD analysis was only possible after multiple depositions to increase the thickness. A wide (111) peak corresponding to a cubic structure was observed for the multiple deposition film. However, the peak position is shifted from the typical position of 28.5671 (PDF card 65-9585) to 29.1851; similar results were reported by Oliva et al. [89] and Chen et al. [90]. The XRD pattern for the as-deposited film only shows a wide diffraction peak. There is also no obvious diffraction peak for the ZnS film at different concentration of reagents. This indicates that this ZnS thin were basically amorphous or microcrystalline structure.

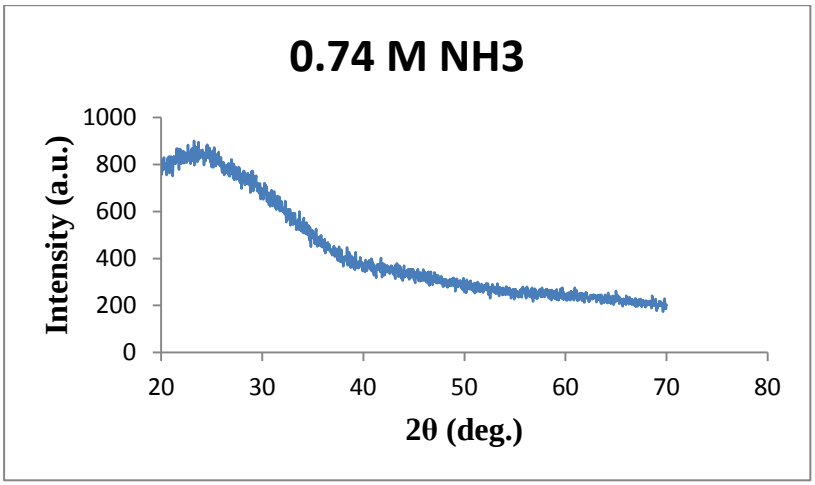

Figure 5.1 X-ray diffraction studies of the ZnS thin Film

5.2 MORPHOLOGY

The patterns of microstructure for the ZnS films were observed by SEM. As shown in Fig. 5, the particles were spherical and homogeneous. However, there were some white spots in the SEM patterns that might be colloidal particles sedimentation mixed with ZnS.

SEM images of as-deposited ZnS thin films prepared using different thiourea concentrations are shown in Fig. 5. It is evident that the films became more uniform and dense with increasing thiourea concentration. The film grown using 0.67 M thiourea consists of small villiform structural grains and has a rough surface. The films grown using 0.83M thiourea are very dense and smooth and have no defined grain boundaries. Thus, the thiourea concentration has no obvious effect on the surface morphology of ZnS thin films.

SEM images of as-deposited ZnS thin films prepared using different ammonia concentrations are shown in **Fig. 5**. It is clear that the ammonia concentration has an obvious effect on the surface morphology of the films. The films grown became denser with increasing ammonia concentration. However, there were some cracks in the thin film deposited using 1.48 M and 2.97 M ammonia. The films deposited using 0.74 M ammonia is more uniform and smoother than the sample prepared using 1.48 M and 2.97 M ammonia. The results can be explained according to kinetics and reaction mechanism for ZnS deposition. The change in the molar NH_3/N_2H_4 ratio resulting from adjustment of the ammonia concentration strongly affects the concentrations of $[Zn(NH_3)_4]^{2+}$, $[Zn(N_2H_4)_3]^{2+}$ and $[Zn(NH_3)_3]^{2+}$ ions. The concentrations of these ions control the rate of Zn^{2+} generation and thus the deposition mechanism for ZnS films. The stability constant for $[Zn(NH_3)_4]^{2+}$, $[Zn(NH_3)_3]^{2+}$ and $[Zn(N_2H_4)_3]^{2+}$ is $10^{8.9}$, $10^{6.6}$ and $10^{5.5}$, respectively [9]. A higher stability constant means that Zn^{2+} release will be slower from these complexes and the rate of ZnS deposition will be very slow. A lower stability constant means that Zn^{2+} release will be faster and thus ZnS and $Zn(OH)_2$ colloidal particles can easily form and precipitate out in the solution. For ammonia concentrations of 0.74 and 1.48M (NH_3/N_2H_4 ratio 0.89 or 1.78), $[Zn(NH_3)_3]^{2+}$ ions play an important role in the deposition process. The larger particles are formed by aggregation of ZnS colloid particles in solution (cluster-by-cluster deposition). By contrast, a few nanometer-sized particles are formed via ion-by-ion reactions on the surface and strongly adhere to it. We can conclude that an optimal NH_3/N_2H_4 ratio is necessary for the formation of high-quality ZnS thin films.

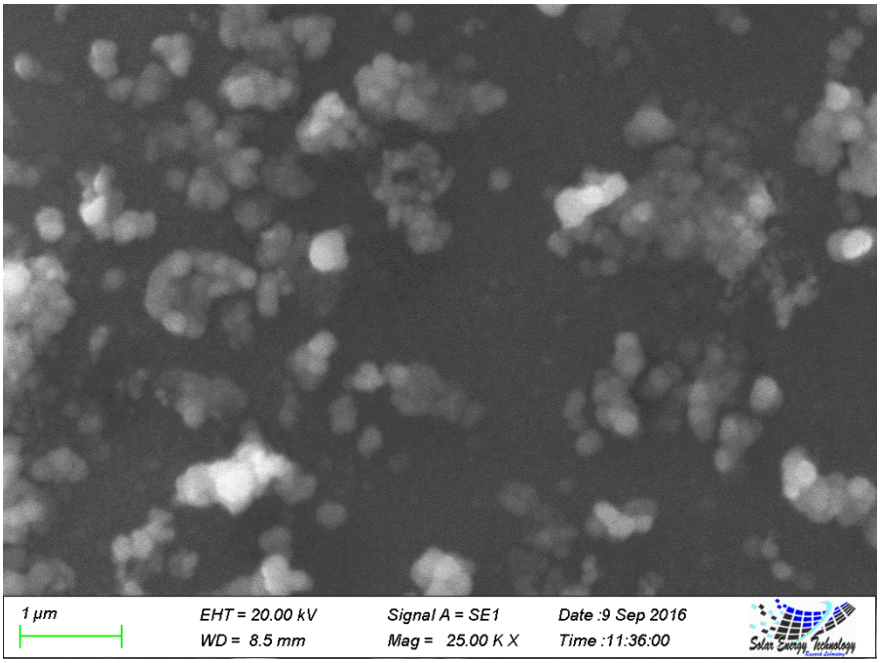

Figure 5.2 SEM image of as-deposited ZnS thin films for 0.74M NH_3

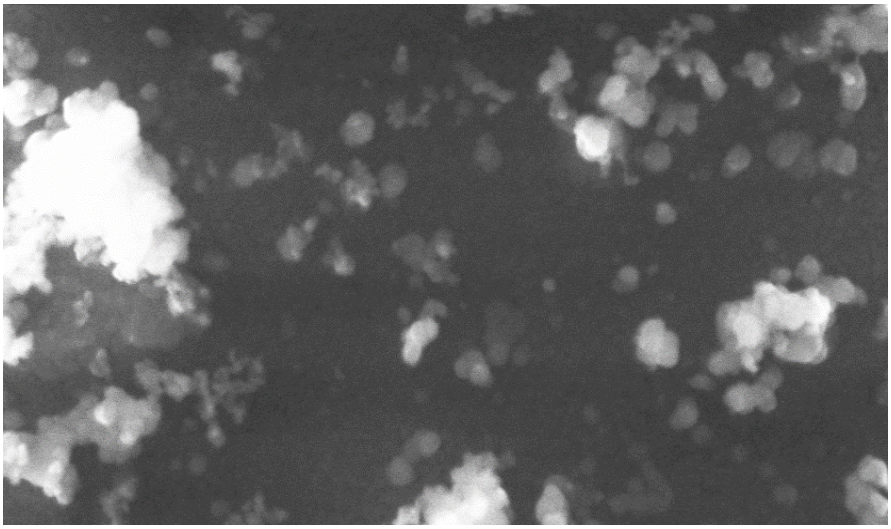

Figure 5.3 SEM image of as-deposited ZnS thin films for 1.48M NH3

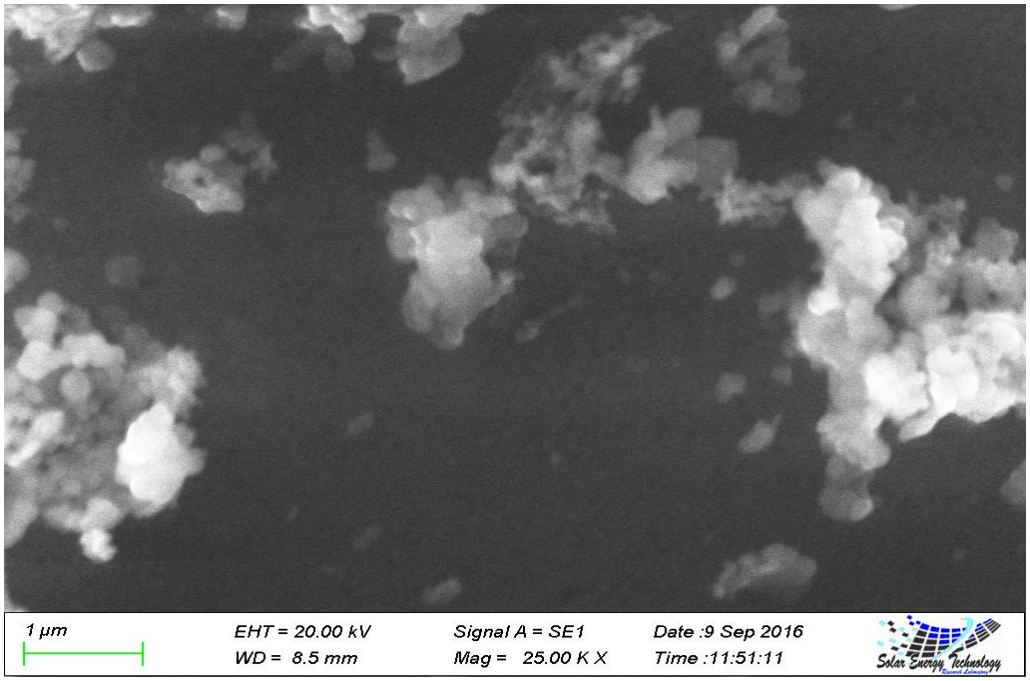

Figure 5.4 SEM images of as-deposited ZnS thin films for 2.97M NH_3

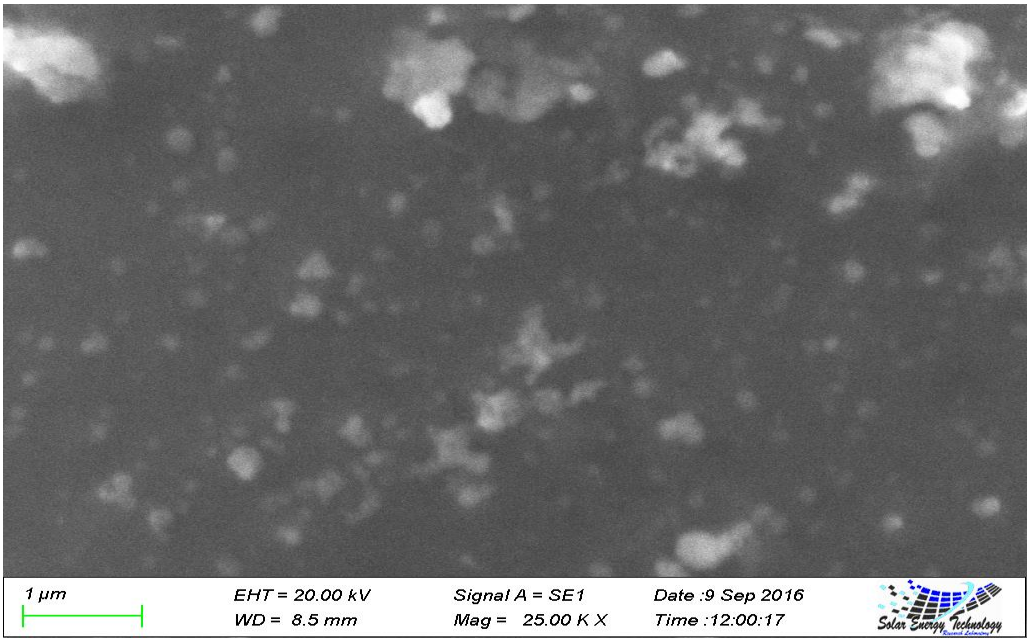

Figure 5.5 SEM image of as-deposited ZnS thin film for 0.67M thiourea [$SC(NH_2)_2$]

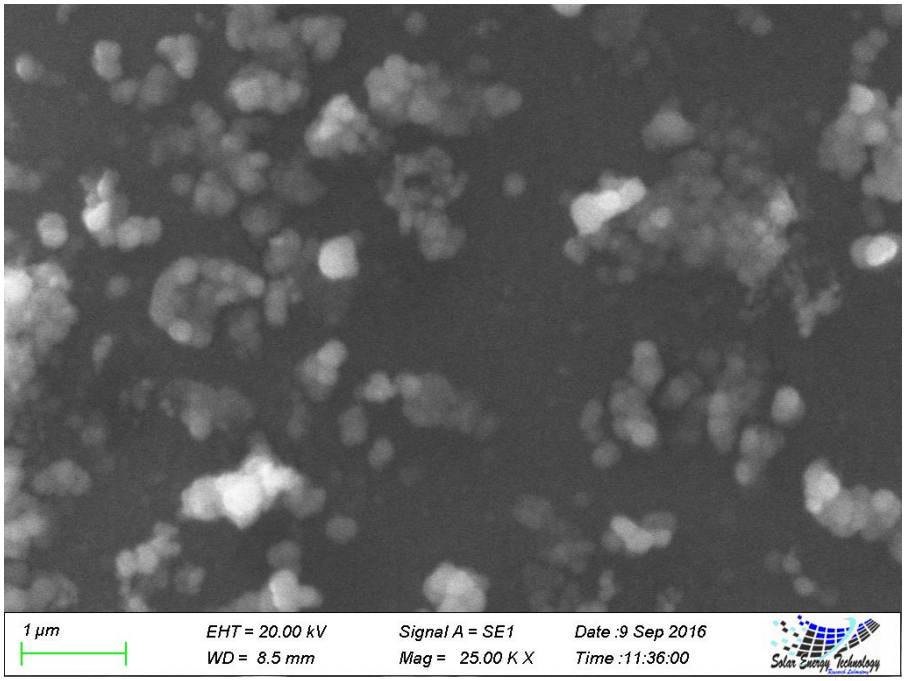

Figure 5.5B SEM images of as-deposited ZnS thin films for 0.83M thiourea [$SC(NH_2)_2$]

5.3 ELEMENTAL ANALYSIS

The sulfur and zinc content in as-deposited ZnS films was determined by EDS analysis. The results are shown in **Table 2**. The results indicate that the thiourea and ammonia concentrations markedly affect the S/Zn ratio in the films. ZnS thin films prepared by CBD were zinc-rich. The coexistence of $Zn(OH)_2$ and ZnO is a possible reason for this.

Hydrolysis of thiourea provides S^{2+} ions, and thus the thiourea concentration affects the concentration of S^{2+} ions during deposition. The composition of S increases in as-deposited ZnS with increasing thiourea concentration. The pH of the reaction solution strongly depends on the ammonia concentration. Before deposition, the pH values for reaction solutions containing 0.74, 1.47 and 2.97 M were 9.3, 9.7, and 10.1 and decreased to 8.3, 8.8, 9.2 and 9.4, respectively, after deposition. The figures show that the amount of Zn and S in as-deposited ZnS thin films is slightly changed for different concentration of ammonia and thiourea. But the amount of Zn is always rich than S in overall ZnS composition. It is possible that several soluble and insoluble Zn^{2+} species exist in aqueous alkaline solution. When the pH of the reaction solution is less than 7.5 or greater than 11.4, soluble species of Zn^{2+} or $ZnO^{2}{}_{2}^{-}$, respectively, are present [91]. At pH 7.5–11.4, insoluble $Zn(OH)_2$ may also be present. This is the reason for the high amount of $Zn(OH)_2$ colloids suspended in the

reaction solutions. Sahraei et al. prepared ZnS thin films in a weak acidic medium as a new CBD route, and obtained films with a composition much closer to stoichiometric ZnS because of significantly lower concentrations of $Zn(OH)_2$ and ZnO species or organic impurities in the films [88].

There is competition between homogeneous and heterogeneous reactions in the formation of ZnS films. Depending on the growth mechanism, $Zn(OH)_2$ colloids may form directly in the reaction bath at lower ammonia concentrations because Zn^{2+} ions are easily released, and thus more $Zn(OH)_2$ may exist in the film. Otherwise, since $Zn(OH)_2$ serves as nuclei in ion-by-ion deposition, it will also probably be present in films if it is not completely consumed during film growth.

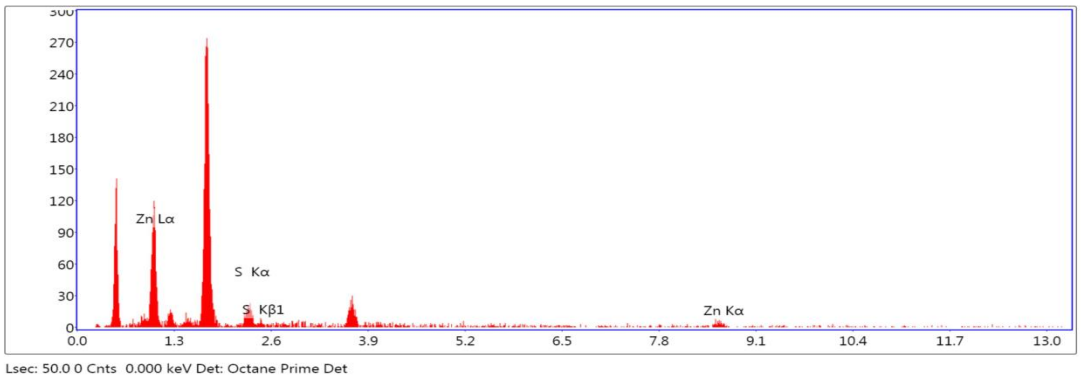

Figure 5.6 EDX elemental analysis of as-deposited ZnS thin films for 0.74M NH_3

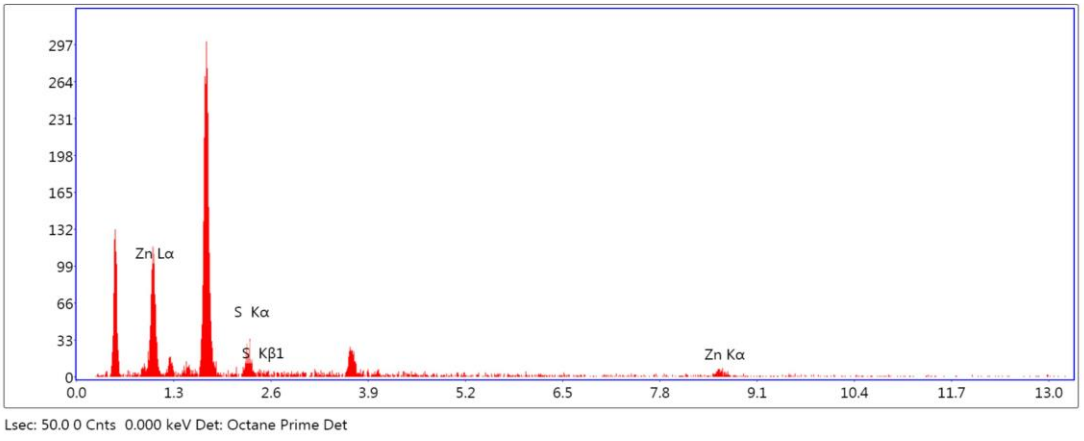

Figure 5.7 EDX elemental analysis ZnS thin films for 1.48M NH_3

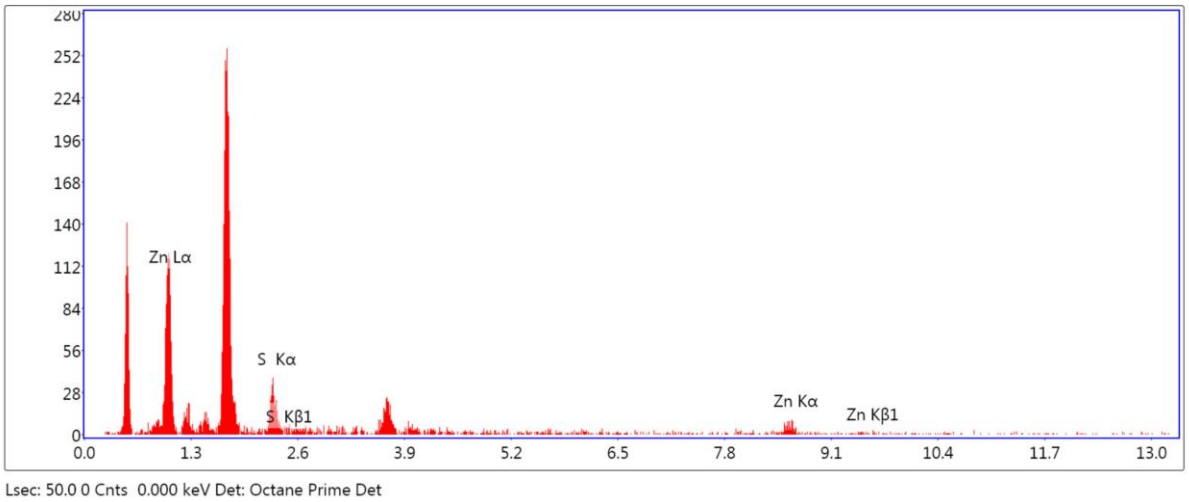

Figure 5.8 EDX elemental analysis of as-deposited ZnS thin films for 2.97M NH_3

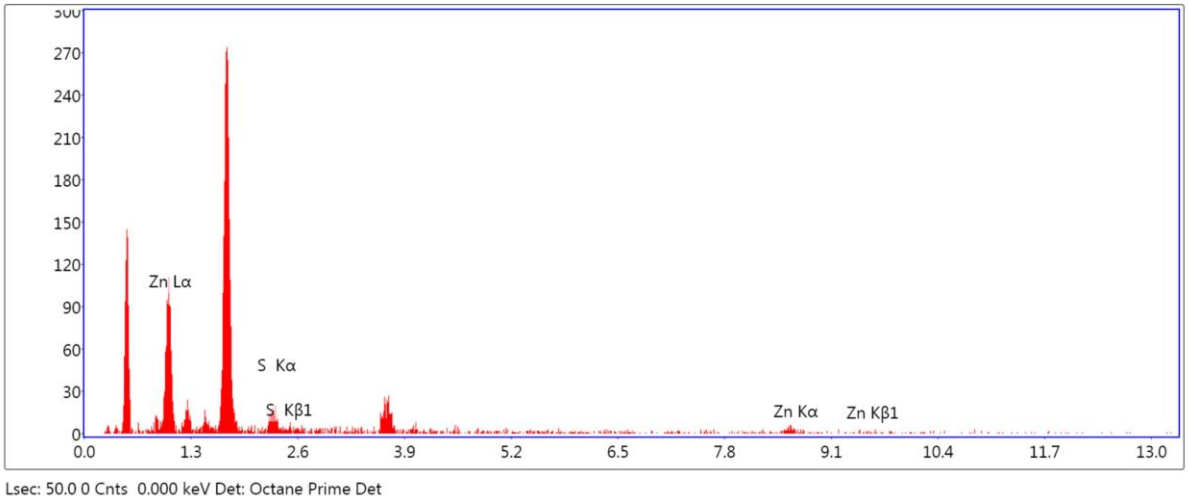

Figure 5.9 EDX elemental analysis of as-deposited ZnS thin films for 0.67M thiourea $[SC(NH_2)_2]$

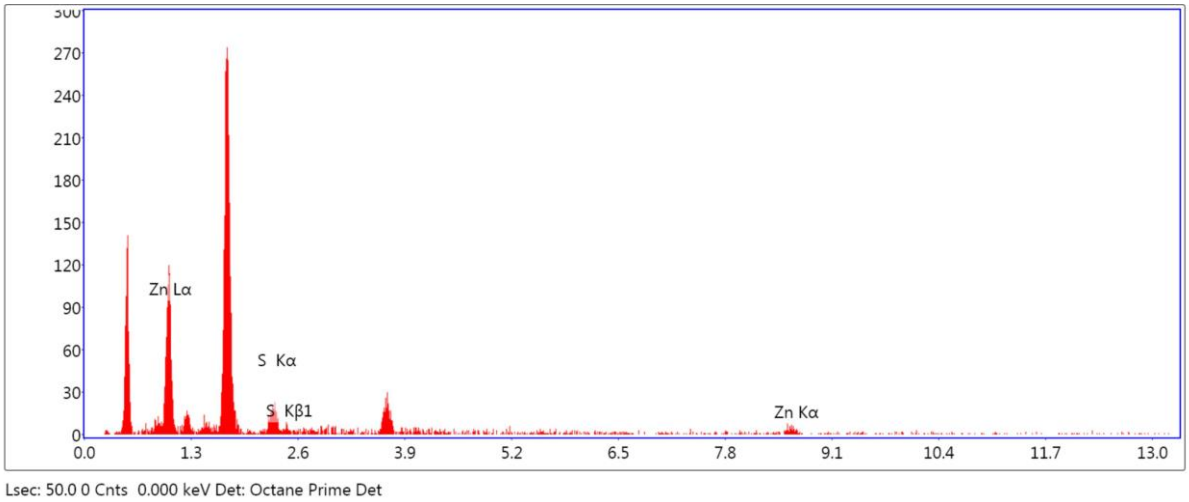

Figure 5.10 EDX elemental analysis of as-deposited ZnS thin films for 0.83M thiourea $[SC(NH_2)_2)$

Table 5.1 Content of S and Zn in as-deposited ZnS films prepared with different thiourea and ammonia concentrations

	Ammonia concentration			Thiourea concentration	
	0.74M	1.48M	2.97M	0.67M	0.83M
S (wt %)	38.9	36	37.7	37	38.9
Zn (wt %)	61.1	64	62.3	63	61.1
S/Zn (ratio)	0.64	0.56	0.61	0.58	0.64
Bandgap(ev)	3.89	3.87	3.85	3.87	3.88

5.4 OPTICAL PROPERTIES AND BAND GAP

5.4.1 TRANSMITTANCE

When light is incident on a material, fraction of the light beam that is not reflected or absorbed is transmitted through the material. The optical properties of ZnS thin films are determined from transmission measurements in the range of 300–1100 nm. Fig. 4 shows the transmission spectra of hexagonal ZnS thin films for different concentrations of ammonia and thiuorea deposited at 70 °C varying from 72 to 319 nm thicknesses. The ZnS films showed

optical transmission 40–65% in the visible range. It is evident from the figure that the transmittance decreases with increasing molar concentration of ammonia and thiourea.

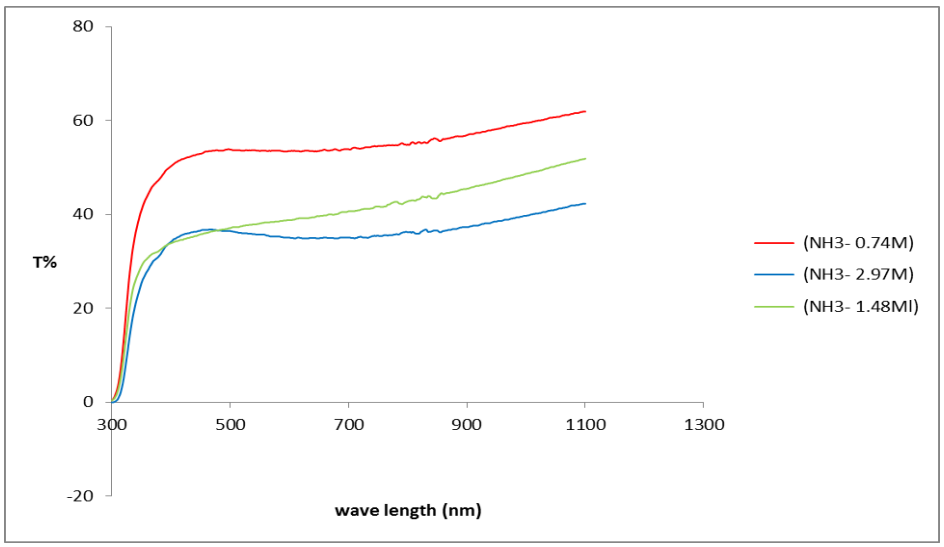

Figure 5.11 Transmittance as function UV-vis wave length for different ammonia concentration

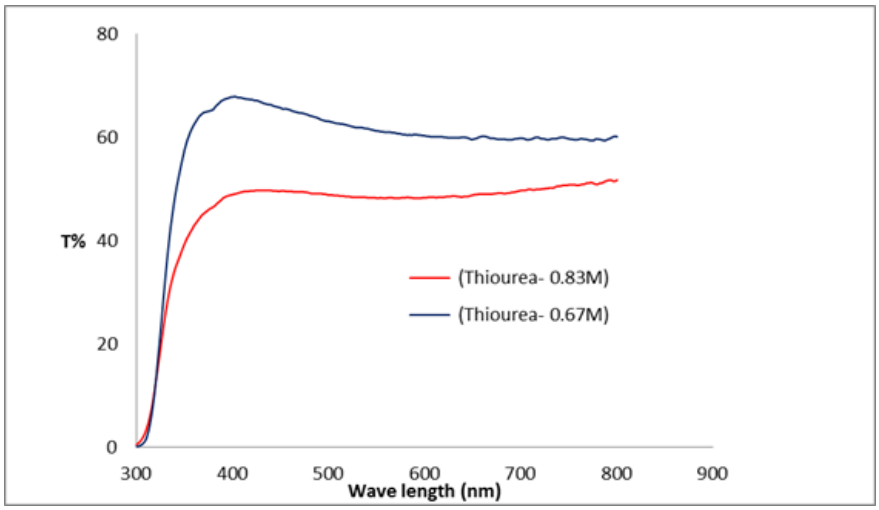

Figure 5.12 Transmittance as function UV-vis wave length for different thiourea concentration

From above graph, it is shown that Transmittance of as-deposited ZnS thin films decreases with the increasing molar concentration of ammonia and thiourea.

5.4.2 ABSORBANCE

The values of absorption coefficient are calculated by the following equation, which is based on the Beer-Lambert law for optical absorption, where film thickness (t), Absorbance (A), and the Absorption coefficient (α) .

$$\alpha = 2.303*A/t$$

As deposited thin films were whitish in colour and adherent. The Figures (5.1A-5.1D) below show the absorption spectra of thin films of ZnS for different ammonia and thiourea concentration.

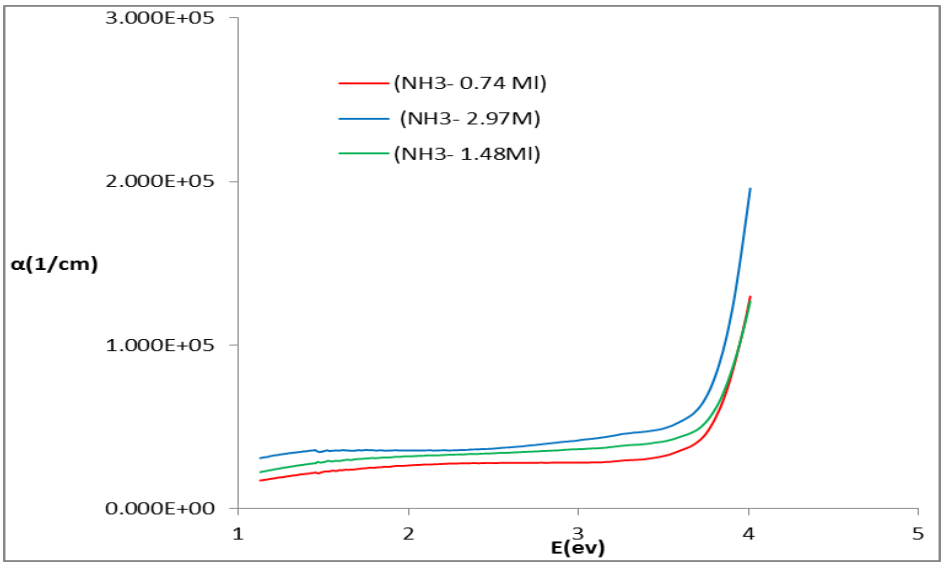

Figure 5.13 A plot of absorption coefficient versus wavelength with different ammonia concentration

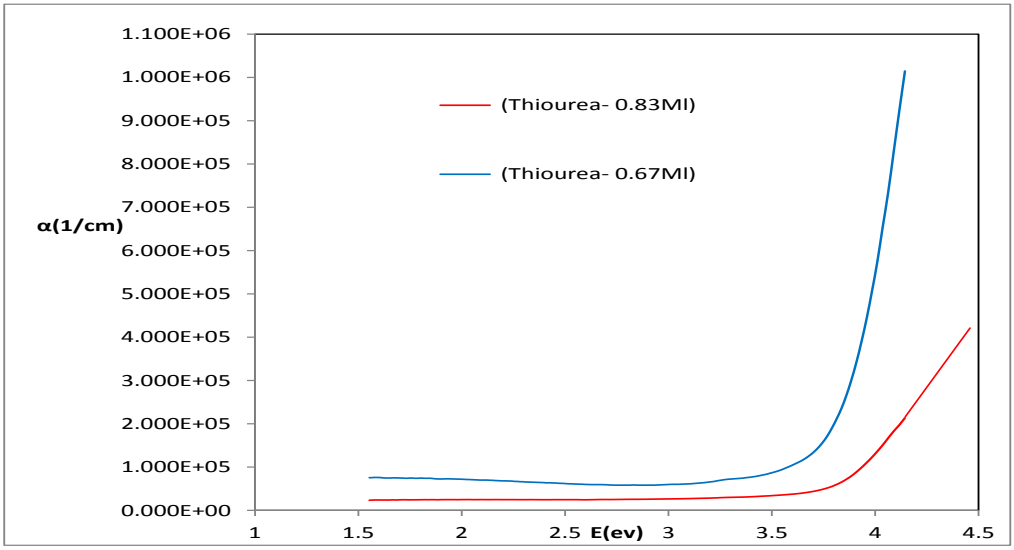

Figure 5.14 A plot of absorption coefficient versus wavelength with different thiourea concentration

From above graph, it is shown that absorbance of as-deposited ZnS thin films increases with the increasing molar concentration of ammonia and thiourea.

5.4.3 OPTICAL BAND GAP

The absorption coefficient, α, of the thin films is calculated from the absorbance spectrum by using the expression;

$$\alpha = 2.303*(A/t) \qquad 5.1$$

Where 'A' is the absorbance and 't' is the thickness of the film.

Almost all the II-VI compounds are direct band gap semiconductors. The optical band gap of the thin films were estimated from absorption coefficient data as a function of wavelength by using the Tauc Relation for direct band gap materials, which is given by

$$\alpha h\nu = A(h\nu - E_g)^{1/2} \qquad 5.2$$

Where hυ, is the photon energy, E_g, the optical band gap and A is a constant.

By plotting a graph of $(\alpha h\upsilon)^2$ as ordinate and hυ as abscissa, the optical band gap E_g can be determined by the extrapolation of best fit line between $(\alpha h\upsilon)^2$ and hυ to intercept the hυ axis at $(\alpha h\upsilon)^2 = 0$. This intercept gives the value of the optical band gap of the material.

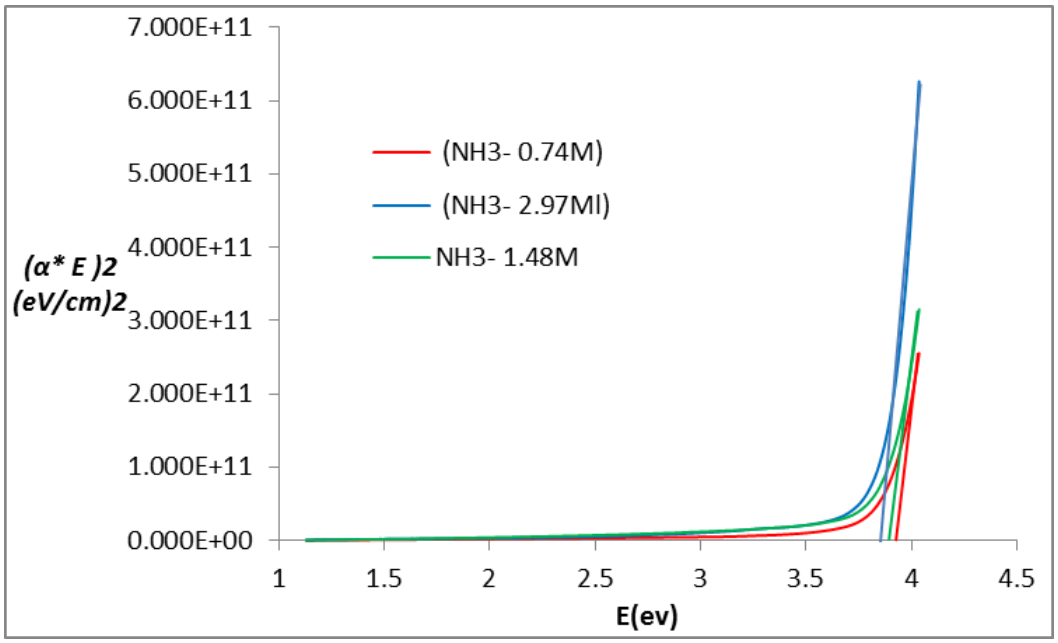

Figure 5.15 $(\alpha h\nu)^2$ versus hν curves for as-deposited ZnS films prepared with different ammonia concentration

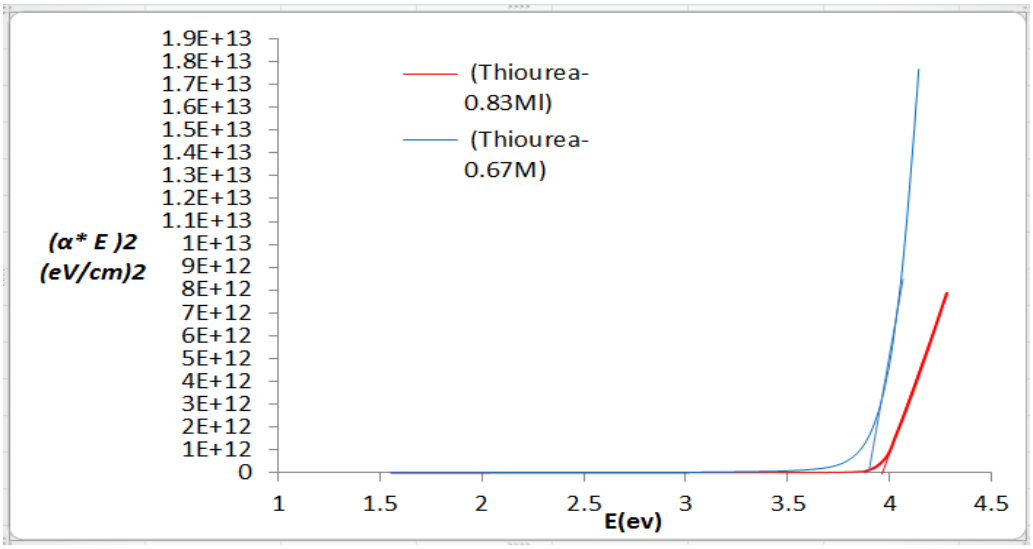

Figure 5.16 $(\alpha h\nu)^2$ versus hv curves for as-deposited ZnS films prepared with different thiourea concentration

Table 5.2 shows $(\alpha h\nu)^2$ versus $(h\nu)$ plots for as-deposited ZnS films prepared at different thiourea and ammonia concentrations. The optical bandgap of ZnS thin films varied in the range 3.85–3.89 eV. The optical bandgap first increased and then decreased with increasing ammonia or thiourea concentration.

Table 5.2 Bandgap for different ammonia and thiourea concentration

	Ammonia concentration			Thiourea concentration	
	0.74M	1.48M	2.97M	0.67M	0.83M
Bandgap(ev)	3.89	3.87	3.85	3.87	3.89

6. CHAPTER SIX

6.0 CONCLUSIONS

ZnS thin films were prepared by CBD on glass substrates using different thiourea and ammonia concentrations. A well adherent thin film of ZnS has been deposited on silica glass substrates containing zinc sulfate ($ZnSO_4$ $7H_2O$), thiourea [$SC(NH_2)_2$], ammonia (NH_3) and hydrazine hydrate (N_2H_4). SEM micrograph of the as-deposited ZnS thin film, show the film to be uniform, dense, homogenous, and composed of largely irregular shaped grains. EDAX results are consistent with the formation of thin films of ZnS deposited on silica glass substrates. The optical absorbance of these films was measured by Schimadzu UV-VIS spectrophotometer within wavelength range of 300-800 nm. It was observed that the absorbance transmittance varies with different ammonia and thiourea concentrations. The molar NH_3/N_2H_4 ratio affected the surface morphology, optical properties and deposition mechanism for ZnS thin films. For a lower NH_3/N_2H_4 ratio, film growth was via a cluster-by-cluster mechanism. For a larger NH_3/N_2H_4 ratio, the predominant growth mechanism was an ion-by-ion process. For a moderate NH_3/N_2H_4 ratio (e.g., 0.49), the two distinct growth mechanisms coexisted. The atomic S/Zn ratio for films deposited under optimal conditions was 0.64. The coexistence of $Zn(OH)_2$ and ZnO is a possible reason for this zinc-rich composition. The optical transmittance of ZnS thin films was 64% in the wavelength range 300–1100 nm. The optical bandgap calculated from transmission spectra was 3.85–3.89 eV. ZnS thin films obtained by CBD showed poor crystallinity. The optimal conditions for deposition of high-quality ZnS thin films were a thiourea concentration of 0.75 M and a molar NH_3/N_2H_4 ratio of 0.8–1.2.

6.1 FUTURE WORK

It has been recognised from various earlier works that ZnS adopts cubic crystal structure whenever its fabrication is done in chemical methods. It has also been shown that this phase of ZnS exhibits lattice mismatch with respect to the various popular absorber layer materials e.g. CZT etc. This again generates copious trap centers which are the major contributor to efficiency-loss involving recombination of the photo-generated charge carriers before reaching the junction. In this respect other absorber layer materials has to be explored for the further understanding of the interfacial environment of ZnS with respect to the absorber layer. In future hetero junction and homo junction characteristics will be investigated with reference to various absorbers. There is a huge future prospect for the detailed study of this method as far as fabrication of ZnS thin film is concerned such as:

1. ZnS thin film analysis (structural, morphological, optical) with different annealing temperature, different deposition time (from 10 min to 5 hours).
2. Electrical analysis (conductivity, resistivity) of as-deposited ZnS thin film.
3. Electron Diffraction measurements to ascertain whether the samples are amorphous or polycrystalline.
4. Hall Effect measurements should be carried out to determine the conductivity type.

REFERENCES

[1] Young, H.D. and Freedman, R.A., (2008). *University Physics with Modern Physics*, 12th Edition, pp. 1449-1455.

[2] Tan W.C. (2006). *Optical properties of amorphous selenium films* Thesis University of Saskatchewan, pp. 3-13

[3] Vipin, K., Sharma, M.K., Gaur, J., Sharma, T.P., (2008). Polycrystalline Zns Thin Films By screen Printing Method And Its Characterization, *J chalcogenide Letters Vol.5, No 11:p 289, 291*.

[4] Gilbert B., Frazer B. H., Zhang H., Huang F., Banfield J. F., Haskel D., Lang J. C., Srajer G., De Stasio G. (2002). Quoted by Nasra B. T., Kamouna N., Kanzari M., Bennaceur R., (2006). Effect of pH on the properties of ZnS thin films grown by chemical bath deposition. *Journal of Thin Solid Films,* 500, pp 4 – 8

[5] Greenwood N. and Earnshaw A., (1984). *Chemistry of the Elements,* Oxford: Pergamon, p. 1405, ISBN 0-08-022057-6

[6] Blos, W.H.N., Pfisterer , F., Shock, H.W., (1998). Quoted by Boyle, D.S., Robbe, O., Hallida, D.P., Heinrich, M.R., Bayer, A. ,O'Brien, Otway, D.J. and Potter, M.D.G., (2000). *Journal of Material Communication Chemistry*.

[7] Katsumi K., (1995). Jpn. *J.Appl. Physics,* pp 33,4383. **Li, S.S., (2006).** Semiconductor Physical Electronics, Second Edition, pp.246-253, p.335.

[8] Ndukwe, I.C (1996) *Solar Energy Materials and Solar Cells* , 40,123.

[9] Hasse, M.A., Qui, J., DePuydt, J.M., Cheng, H., (1991*).* *Appl. Phys. Lett*., 59, 1272.

[10] Kashani H., (1996). *Thin solid Films*, 288(1-2).

[11 Ortega, R., Borges, D. (1992). *Lincot and Vedel, in Proc. 11th ed. E.C Photovoltaic solar Energy Conf* **.,** Hawood Academic Publishers, Switzerland,p862.

[12] Yamaga S., Yoshokawa A. and Kasain H.,(1998). Cited in K. R. Murali, and S. Kumaresan. (2009). Characteristics of Brush Plated ZnS Films *Chalcogenide Letters* Vol. 6, (1), pp. 17 –22

[13] Kassim, A., Nagalingam, .S.,Tee T.W., sharif, A.M., Abdulah, D. K., Elos M. J and Min, H.S., (2009). Effect Deposition Period and PH on Chemical Deposition Cuns4 thin Films, *Philipians Journal of science* 138(2): 161-168.

[14] Singh, J., (2006). Optical Properties of Condensed Matter and Applications, *John Wiley and Sons, Ltd*. pp.2-4.

[15] Zainal Z., Zobir Hussein M., Ghazali A., (1996). Solar Energy Materials and Solar Cells, **40**, 347

[16] Petterson, J. D. and Bailey, B. C., (2005). Solid-State Physics Introduction to the Theory, pp.293-294, 113, 637.

[17] Ohring, M., (1992). The Materials Science of Thin Films, *Academic Press*, San Diego.pp. 195-199, 336-339.

[18] Ilenikhena P. A., (2008). Comparitive Studies of Improved Chemical Bath Deposited Copper Sulphide (CuS) and Zinc Sulphide (ZnS) Thin Films at 320K and Possible Applications. *Journal of African Physical Review*, **2**: 0007 59

[19] Nadeem, .M.Y., Ahmed,W.(2000), Turk. *J.Phys*., 24651

[20] Hammer K., (1943). *Z. Techn. Phys.*, 24, 169p

[21] Huldt and Staflin, Gonellian. Cited in Nadeem, M.Y., Ahmed, W., Wasiq M.F., (2005). ZnS Thin Films – An Overview . *J of Research (science) ; Buhauddin Zakaniya University, Multan, Pakistan*-Vol.16, pp105.

[22] Polster, H.D (1952). J. Opt. soc. Amer. 42, 4

[23] Nadeem M.Y., Ahmed W., Wasiq M.F., (2005). ZnS Thin Films – An Overview . *J of Research (science) ; Buhauddin Zakaniya University, Multan, Pakista*n-Vol.16, pp105.

[24] Yamaguchi, T., Yamamoto, Y., Tanaka, T., Demizu, Y. and Yoshida, A., (1996). *Thin Solid Films*, **281/282**, 375.

[25] Lindroos, S., Kannianen, Tapio., Leskela,M.(1997) Quoted by Nadeem, M.Y., Ahmed, W., Wasiq M.F., (2005). ZnS Thin Films – An Overview . *J of Research (science) ; Buhauddin Zakaniya University, Multan, Pakistan*-Vol.16, pp105.

[26] Gomezdaza A., Sanchez O., A., Campos J., Hu H., Suarez R., Rincón M. F., (1998), Sol. Energy *Mat. Sol. Cells*, 52, 313.

[27] Nair P. K.,Nair M. T. S., Garcıa V. M., Arenas O. L., Pena Y., Castillo A., Yala I. T.

[28] Johnston D. A., Carletto M. H., Reddy K. T. R, Forbes I. and Miles R., (2002). W. *Thin Solid Films.* 403-404 102-6

[29] Padam G. K., Rao S. U. M. and Maholtra G. L. (1988), *J. Appl. Phys*., 63, 770

[30] O'Brien P. and McAleese J., (1998). Quoted by Jie Cheng, DongBo Fan, Hao Wang, BingWei Liu, YongCai Zhang and Hui Yan. Chemical bath deposition of crystalline ZnS thin films. *Journal of Semicond. Sci. Technol.* 18 No 7 (July 2003) 676-679 PII: S0268-1242(03)58148-2

[31] Edelson, V (2007). *Concentration Crisis.* In Brown Alumni Magazine, July/August 2007

[32] P. Roy, J.R. Ota, S.K. Srivastava, Thin Solid Films 515 (2006) 1912–1917.

[33] F. Long, W.M. Wang, Z. Cui, L.Z. Fan, Z. Zou, T. Jia, Chem. Phys. Lett. 462 (2008) 84–87.

[34] G.L. Agawane, S.W. Shin, A.V. Moholkar, K.V. Gurav, J.H. Yun, J.Y. Lee, J.H. Kim, J. Alloys Compd. 535 (2012) 53–61.

[35] W. Vallejo, C. Quiñones, G. Gordillo, J. Phys. Chem. Solids 73 (2012) 573-578.

[36] J.M. Dona, J. Herrero, J. Electrochem. Soc. 141 (1994) 205–210.

[37] J. Vidal, O. Vigil, O. De Melo, N. Lopez, O. Zelaya-Angel, Mater. Chem. Phys. 61 (1999) 139–142.

[38] I.O. Oladeji, L. Chow, Thin Solid Films 474 (2005) 77–83.

[39] S.M. Salim, A.H. Eid, A.M. Salem, H.M.A.b.o.u. El-Kair, Surf. Interface Anal. 44 (2012) 1214–1218.

[40] P. O'Brien, J. McAleese, J. Mater. Chem. 8 (1998) 2309–2314.

[41] R. Sahraei, G.M. Aval, A. Baghizadeh, M. Lamehi-Rachti, A. Goudarzi M.H. Majles Ara, Mater. Lett. 62 (2008) 4345–4347.

[42] K. Yamaguchi, T. Yoshida, D. Lincot, H. Minoura, J. Phys. Chem. B. 107 (2003) 387–397.

[43] M. Kostoglous, N. Andritsos, A.J. Karabelas, J. Colloid. Interface Sci. 263 (2003) 177–189.

[44] A. Goudarzi, G.M. Aval, R. Sahraei, H. Ahmadpoor, Thin Solid Films 516 (2008) 4953–4957.

[45] S.S. Kawar, B.H. Pawar, Micro Nano Lett. IET 5 (2010) 100–104.

[46] Y. Zhang, X.Y. Dang, J. Jin, T. Yu, B.Z. Li, Q. He, F.Y. Li, Y. Sun, Appl. Surf.Sci. 256 (2010) 6871–6875.

[47] S.R. Kang, S.W. Shin, D.S. Choi, A.V. Moholkar, J.H. Moon, J. Kim, Curr. Appl. Phys. 10 (2010) S473–S477.

[48] S.W. Shin, G.L. Agawane, M.G. Gang, A.V. Moholkar, J.H. Moon, J. H. Kim, J.Y. Lee, J. Alloys Compd. 526 (2012) 25–30.

[49] A.X. Wei, X.H. Zhao, J. Liu, Y. Zhao, Physica B 410 (2013) 120–125.

[50] Neamen, D.A., (2003). Semiconductor Physics and Devices, Basic Principles, Third Edition, p.2, pp. 144-145.

[51] Yacobi, B. G., (2004). Semiconductor Materials: An Introduction to Basic Principles, pp.1-3, 154-157, 107.

[52] Singh, J., (2003). Electronic and Optoelectronic Properties of Semiconductor Structures, *Cambridge University Press*; New York, p. IV, 51-52.

[53] Korvink, J. G. and Greiner, A., (2002). Semiconductors for micro and Nano technology an Introduction for engineers, p.40.

[54] Yewu Wang, Lide Zhang, Changhao Liang, Guozhong Wang, Xinsheng Peng; Catalytic growth and photoluminescence properties of semiconductor single-crystal ZnS nanowires; Chemical Physics Letters 357 (2002) 314–318

[55] F. Godea, C. Gumus, M. Zor; Investigations on the physical properties of the polycrystalline ZnS thin films deposited by the chemical bath deposition method; Journal of Crystal Growth 299 (2007) 136–141

[56] A. F. Shchurov, V. A. Perevoshchikov, T. A. Gracheva, N. D. Malygin, D. Shevarenkov, E. M. Gavrishchuk, V. B. Ikonnikov, and E. V. Yashina; Structure and Mechanical Properties of Polycrystalline Zinc Sulfide; N. *Inorganic Materials, Vol. 40, No. 2, 2004, pp. 96–101*

[57] Anderson, F. (1959), Acta Chem Scond 8 pp. 1599. Cited by Madon A. and Shaw M. P., (1988). The Physics and Application of Amorphous Semiconductors. *Academic Press Inc. London*

[58] Kittel, C., (2005). Introduction to Solid State Physics, Eighth Edition. *John Wiley & Sons, Inc*. p.577

[59] Ben G. Streetman; Solid State Electronic Devices.

[60] Xiaochun Wu, Fachun Lai, Limei Lin, Jing Lv, Binping Zhuang, Qu Yan, Zhigao Huang; Optical inhomogeneity of ZnS films deposited by thermal evaporation; Applied Surface Science 254 (2008) 6455–6460

[61] H.J. Yuan, S.S. Xie, D.F. Liu, X.Q. Yan, Z.P. Zhou, L.J. Ci, J.X. Wang, Y. Gao,L. Song, L.F. Liu, W.Y. Zhou, G. Wang; Formation of ZnS nanostructures by a simple way of thermal evaporation; Journal of Crystal Growth 258 (2003) 225–231

[62] Le-Xi Shao, Kuen-Huei Chang, Huey-Liang Hwang; Zinc sulfide thin films deposited by RF reactive sputtering for photovoltaic applications; Applied Surface Science 212–213 (2003) 305–310

[63] Prof. Biswajit Ghosh; Fundamentals of Solar Electricity; Jadavpur University, 2009

[64] K.T. Hillie, C. Curren, H.C. Swart; ZnS thin films grown on Si(100) by XeCl pulsed laser ablation: Applied Surface Science 177 (2001) 73-77

[65] Gilbert B., Frazer B. H., Zhang H., Huang F., Banfield J. F., Haskel D., Lang J. C.,

[66] R. R. Chamberlin and J.S. Skarman. J. Elecrrochem. Sot., 113 (1966) 86.

[67] N. Poornima, Anjaly Jose, C. Sudha Kartha and K.P. Vijayakumar; Composition and Conductivity-type Analysis of Spray Pyrolysed ZnS Thin Films using Photoluminescence; Energy Procedia 15 (2012) 347 – 353

[68] B. Elidrissi, M. Addoua, M. Regragui, A. Bougrine, A. Kachouane, J.C. Bernède; Structure, composition and optical properties of ZnS thin films prepared by spray pyrolysi; Materials Chemistry and Physics 68 (2001), 175–179

[69] P. Biswas, R. Senthil Kumar, P. Ramavath, V. Mahendar, G.V.N. Rao, U.S. Hareesh, R. Johnson; Effect of post-CVD thermal treatments on crystallographic orientation, microstructure, mechanical and optical properties of ZnS ceramics; Journal of Alloys and Compounds 496 (2010) 273–277

[70] N.H. Tran, R.N. Lamb, G.L. Mar; Single source chemical vapour deposition of zinc sulfide thin films film composition and structure; Colloids and Surfaces

[71] Everett Y.M. Lee, Nguyen H. Tran, Robert N. Lamb; Growth of ZnS films by chemical vapor deposition of Zn[S2CN(CH3)2]2 precursor; Applied Surface Science 241 (2005) 493–496

[72] Beer Pal Singh, Virendra Singh, R.C. Tyagi, T.P. Sharma; Effect of ambient hydrogen sulfide on the physical properties of vacuum evaporated thin films of zinc sulfide; Applied Surface Science 254 (2008) 2233–2237

[73] Nicolau YF. Appl Surf Sci 1985;22/23:1061

[74] Aytunc Ates, M. Ali, Yıldırım, Mutlu Kundakcı, Aykut Astam; Annealing and light effect on optical and electrical properties of ZnS thin films grown with the SILAR method; Materials Science in Semiconductor Processing 10 (2007) 281– 286

[75] Ian Y.Y. Bu; Sol–gel synthesis of ZnS (O,OH) thin films: Influence of precursor and process temperature on its optoelectronic properties; Journal of Luminescence 134 (2013) 423–428

[76] N.I. Kovtyukhova, E.V. Buzaneva, C.C. Waraksa, T.E. Mallouk; Ultrathin nanoparticle ZnS and ZnS: Mn films: surface sol–gel synthesis, morphology, photophysical properties; Materials Science and Engineering B69–70 (2000) 411–417

[77] Poulomi Roy, Jyoti R. Ota, Suneel Kumar Srivastava; Crystalline ZnS thin films by chemical bath deposition method and its characterization; Thin Solid Films 515 (2006) 1912–1917

[78] N. Kamoun Allouchea, T. Ben Nasra, N. Turki Kamouna, C. Guaschb; Synthesis and properties of chemical bath deposited ZnS multilayer films; Materials Chemistry and Physics 123 (2010) 620–624

[79] Tetsuya Miyawaki, Masaya Ichimura; Fabrication of ZnS thin films by an improved photochemical deposition method and application to ZnS/SnS heterojunction cells; Materials Letters 61 (2007) 4683–4686

[80] M. Gunasekarana, R. Gopalakrishnana, P. Ramasamy; Deposition of ZnS thin films by photochemical deposition technique; Materials Letters 58 (2003) 67– 70

[81] T. Suntola, J. Antson, US Patent 4058430, 1977

[82] Yong Shin Kim, Sun Jin Yun; Studies on polycrystalline ZnS thin films grown by atomic layer deposition for electroluminescent applications; Applied Surface Science 229 (2004) 105–111

[83] M.A. Contreras, T. Nakada, M. Hongo, A.O. Pudov, J.R. Sites, in: Proceedings of the 3rd World Conference on Photovoltaic Energy Conversion, Osaka, Japan, 2003, pp. 570–573

[84] M.M. Islam, S.Ishizuka, A.Yamada, K.Sakurai, S.Niki, T.Sakurai, K.Akimoto; CIGS solar cell with MBE-grown ZnS buffer layer; Solar Energy Materials & Solar Cells 93 (2009) 970–972

[85] Mattox, D. M., (1978). Surface Cleaning in Thin Film Technology, *Thin Solid Films*, No. 1, **53**, 81.

[86] F. Göde, C. Gümüs, M. Zor, J. Cryst. Growth 299 (2007) 136–141.

[87] M. Lodar, E.J. Popovici, I. Baldea, R. Grecu, E. Indrea, J. Alloys Compd. 434–435 (2007) 697–700.

[88] R. Sahraei, G.M. Aval, A. Goudarzi, J. Alloys Compd. 466 (2008) 488–492.

[89] A.I. Oliva, I. Gonzalez-Chan, V. Rejon, J. Rojas, R. Patino, D. Aguilar, in: Proceedings of the 7th International Conference on Electrical Engineering, Computing Science and Automatic Control, Tuxtla Gutierrez, 2010, pp. 500–503.

[90] Y. Chen, G.F. Huang, W.Q. Huang, L.L. Wang, Y. Tian, Z.L. Ma,

[91] A.M. Chaparro, Chem. Mater. 17 (2005) 4118–4124.